539.128.53/.55

PROPERTIES OF He^3 *AND OF ITS SOLUTIONS IN* He^4

V. N. PESHKOV

Institute of Physics Problems, USSR Academy of Sciences

Usp. Fiz. Nauk 94, 607–640 (April 1968)

CONTENTS

INTRODUCTION

UNTIL recently, He^3 could be observed only in the form of individual atoms in a cloud chamber or with the aid of a mass spectrometer of high resolution. Helium extracted from the atmosphere contains only 10^{-4}% of He^3, and the content in helium from gas sources is smaller by one order of magnitude. However, after it became possible to produce tritium, which is transformed after beta decay into He^3, in noticeable amounts in atomic reactors, He^3 became accessible to extensive investigations, including in the field of low temperatures.

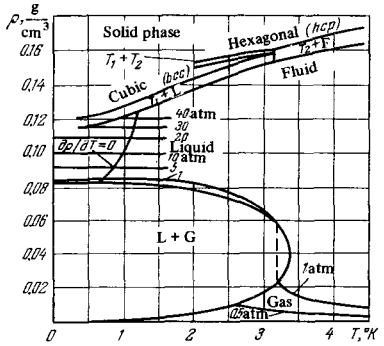

FIG. 1. Temperature dependence of density of He^3.

The low-temperature properties of He^3 have been the subject of more than 700 papers, and there is a number of review articles[1-11] reporting the experimental and theoretical data on He^3 and its solutions in He^4. Naturally, it is impossible to review all these papers in a single article, and we present here only the main characteristics of He^3 and its solutions in He^4, discuss certain features of its properties, connected principally with the quantum nature of liquid helium, and estimate the advantages offered by the use of He^3 to obtain temperatures much lower than 1°K.

1. GENERAL PROPERTIES. ρ–T, p–T, and ν–T DIAGRAMS

In its general properties, He^3 is very similar to He^4, but since its nuclear spin is $\frac{1}{2}$ and its magnetic moment is 1.07×10^{-23} erg/G (0.7618 of the proton moment), it has a number of distinguishing features at low temperatures. Since He^3 has the lightest nucleus of all the noble gases, and the interaction between its atoms is the smallest, it is the last of the gases to turn liquid, and has the lowest atomic density in the liquid state. This density is almost one-third that of hydrogen and smaller by a factor of 1.3 than that of He^4. The temperature dependence of the density of He^3 under phase-equilibrium conditions and for certain pressures of the liquid and gas phases is shown in Fig. 1. The curves

were plotted from the data of Kerr,[12] Peshkov,[13] Grilly and Mills,[14] Rives and Meyer,[15] and Walker and Fairbank.[16]

As seen from the figure, in the liquid phase at saturated vapor pressure in the case of 0.5°K, and at higher pressures in the case of higher temperatures, maxima of the density ($\partial\rho/\partial T \approx 0$) are observed, leading to a sharp decrease of the thermal convection and, consequently to an appreciable decrease of the heat transfer—a very unpleasant effect that must be coped with when working with He^3. He^3, just like He^4, remains liquid down to absolute zero. At low pressures, three phases of solid helium were observed: body centered cubic (bcc), hexagonal close packed (hcp), and face centered cubic (fcc). The triple point of coexistence of liquid and the two solid phases is at T = 3.15°K and p = 140 atm. Figure 2 shows the p–T diagram of He^3 and He^4. It is seen from this diagram that at still higher temperatures and pressures transitions to the fcc solid phase are observed in solid He^3 and He^4. According to Shuch and Mills,[17] the triple points of the transitions are at T = 15.98°K and p = 1341 atm for He^3 and at T = 14.9°K and p = 1100 atm for He^4.

The density of liquid solutions of He^3 and He^4 was measured by Ptukha.[18] According to her data, it is the densities that are approximately additive, $\rho_\nu = \rho_3\nu + \rho_4(1-\nu)$, and not the molar volumes, as should be the case for ideal solutions. Here ρ_ν is the density of a solution with He^3 molar concentration $\nu = He^3/(He^3 + He^4)$, ρ_3 is the density of He^3, and ρ_4 is the density of He^4. The temperatures and pressures are in this case the same. In Fig. 2, the vapor-pressure curves end at critical points, which, according to the measurements,[13, 19] correspond to T_c = 5.20°K and p_c = 2.26 atm for He^4 and T_c = 3.38°K and p_c = 1.22 atm for He^3. The curve of transition of liquid He^4 from the superfluid state into the normal state, the so-called λ line, goes from T_λ = 2.172°K and p_λ = 37.8 mm Hg—the saturated vapor pressure[20]—to an intersection with the crystallization curve at T_λ = 1.765°K and p_λ = 29.9 atm.[21] The vapor-pressure curves on Fig. 2 are based on the internationally accepted temperature scale of 1958 (T_{58}) for He^4[22] and on the 1962 temperature scale[23] for He^3. The temperature scale for He^3 has been determined from 0.2°K to the critical point and corresponds to the equation

$$\ln p_3 = \frac{-2.49174}{T} + 4.80386 - 0.286001T + 0.198608T^2 - 0.0502237T^3 + 0.00505486T^4 + 2.24846\ln T,$$

where p_3 is the pressure in mm Hg at 0°C and at a gravitational acceleration g = 980.665 cm/sec². Table I gives the vapor tension of He^3 on the basis of the foregoing formula, but recalculated to 20°C and to an acceleration 981.56 cm/sec².

The melting curve of He^3 is represented in the interval from 1 to 3.15°K (the phase transition of the solid He^3 from the cubic into the hexagonal phase) by the equation

$$p = 24.559 + 16.639T^2 - 2.0659T^3 + 0.11212T^4,$$

where p is the pressure in atmospheres. According to the authors of [24], the standard deviation from this formula is 0.061 atm.

Figure 3 shows the T–ν diagram of He^3 and He^4. The liquid-vapor equilibrium curves at temperatures above

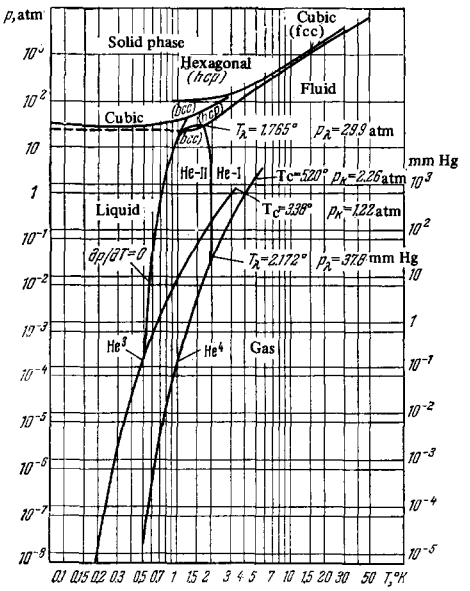

FIG. 2. p–T diagram of He^3 and He^4.

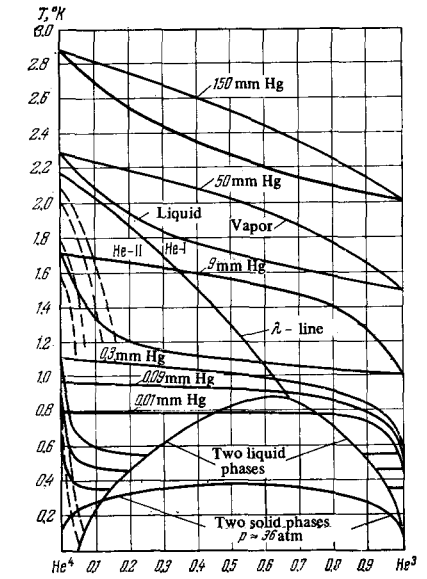

FIG. 3. T – ν diagram of He^3 and He^4.

1.5°K are presented in accordance with the experimental data of [25-28]. At lower temperatures, the curves are only tentative and were obtained on the basis of the assumption that $p = ap_3\nu + p_4(1-\nu)$ and $\nu_v = ap_3\nu/p$, where p is the vapor pressure over a liquid in which the molar concentration of He^3 is equal to ν; p_3 and p_4 are respectively the pressures of pure He^3 and He^4 at this temperature; ν_v is the concentration of He^3 in the vapor phase and a is a constant that varies from 1.2 at T = 2.1° to a = 4 at 1°K and a = 7 at 0.6°K. Approximately such a dependence can be proposed on the basis of the work of Sommers.[27]

The equilibrium curves between two liquid phases* at saturated-vapor pressure are based on experimental data.[28-32] The equilibrium curves between the solid

*On the basis of the latest data [147] the concentration of He^3 along the dissolution curve at $T < 0.15$°K is given by the equation $\nu = 0.0637(1 + 10.8T^2)$.

Table I. Vapor tension of He^3 in accordance with the T_{62} temperature scale[23]

T, °K	0.000	0.005	0.010	0.015	0.020	0.025	0.030	0.035	0.040	0.045	0.050	0.055	0.060	0.065	0.070	0.075	0.080	0.085	0.090	0.095
Pressure in microns mercury																				
0.2	0.0121	0.0173	0.0245	0.0339	0.0464	0.0628	0.0837	0.1106	0.1445	0.1869	0.2394	0.3040	0.3829	0.4784	0.5933	0.7306	0.8935	1.0859	1.3118	1.5755
0.3	1.8821	2.2361	2.6432	3.1104	3.6429	4.2485	4.9344	5.7085	6.5788	7.5535	8.6424	9.8557	11.203	12.695	14.343	16.159	18.154	20.341	22.735	25.347
0.4	28.191	31.285	34.640	38.273	42.200	46.438	51.002	55.912	61.183	66.834	72.884	79.351	86.256	93.616	101.45	109.79	118.64	128.03	137.98	148.52
0.5	159.66	171.42	183.84	196.93	210.71	225.21	240.46	256.48	273.29	290.91	309.38	328.71	348.94	370.08	392.17	415.23	439.28	464.35	490.48	517.67
Pressure in millimeters																				
0.6	0.5460	0.5754	0.6060	0.6377	0.6707	0.7049	0.7404	0.7772	0.8153	0.8547	0.8955	0.9377	0.9814	1.0265	1.0730	1.1212	1.1709	1.2221	1.2749	1.3294
0.7	1.3855	1.4433	1.5029	1.5641	1.6272	1.6920	1.7587	1.8272	1.8977	1.9700	2.0443	2.1205	2.1988	2.2791	2.3614	2.4459	2.5324	2.6211	2.7120	2.8051
0.8	2.9004	2.9979	3.0978	3.2000	3.3045	3.4114	3.5207	3.6324	3.7466	3.8632	3.9824	4.1041	4.2284	4.3553	4.4849	4.6171	4.7519	4.8895	5.0298	5.1729
0.9	5.3188	5.4675	5.6191	5.7736	5.9309	6.0912	6.2544	6.4207	6.5899	6.7623	6.9376	7.1161	7.2977	7.4825	7.6704	7.8616	8.0560	8.2536	8.4546	8.6588
1.0	8.8661	9.0776	9.2922	9.5098	9.7304	9.9552	10.184	10.415	10.651	10.890	11.132	11.379	11.629	11.882	12.139	12.401	12.666	12.933	13.206	13.483
1.1	13.762	14.046	14.334	14.626	14.921	15.221	15.526	15.834	16.146	16.462	16.783	17.106	17.435	17.768	18.105	18.446	18.792	19.142	19.496	19.855
1.2	20.218	20.585	20.957	21.333	21.714	22.099	22.489	22.884	23.283	23.686	24.094	24.507	24.925	25.348	25.774	26.206	26.643	27.084	27.531	27.982
1.3	28.437	28.898	29.365	29.835	30.311	30.792	31.278	31.768	32.265	32.765	33.271	33.783	34.299	34.820	35.348	35.880	36.418	36.960	37.509	38.061
1.4	38.621	39.184	39.754	40.329	40.910	41.496	42.087	42.684	43.286	43.895	44.509	45.128	45.753	46.384	47.021	47.662	48.310	48.964	49.624	50.288
1.5	50.960	51.637	52.320	53.009	53.704	54.405	55.110	55.823	56.542	57.267	57.997	58.734	59.477	60.227	60.982	61.743	62.512	63.286	64.066	64.853
1.6	65.645	66.444	67.250	68.063	68.881	69.705	70.536	71.375	72.218	73.069	73.927	74.790	75.660	76.538	77.421	78.311	79.208	80.111	81.022	81.939
1.7	82.863	83.793	84.731	85.675	86.626	87.585	88.549	89.521	90.499	91.486	92.479	93.479	94.485	95.499	96.520	97.548	98.582	99.625	100.68	101.73
1.8	102.79	103.87	104.94	106.03	107.12	108.22	109.33	110.45	111.57	112.70	113.84	114.98	116.13	117.29	118.46	119.63	120.82	122.01	123.20	124.41
1.9	125.62	126.84	128.07	129.31	130.55	131.80	133.06	134.33	135.60	136.89	138.18	139.48	140.78	142.10	143.42	144.75	146.09	147.43	148.79	150.15
2.0	151.52	152.90	154.29	155.68	157.09	158.50	159.92	161.35	162.78	164.23	165.68	167.14	168.61	170.09	171.58	173.07	174.58	176.09	177.61	179.14
2.1	180.67	182.22	183.77	185.34	186.91	188.49	190.08	191.68	193.28	194.90	196.52	198.16	199.80	201.45	203.11	204.78	206.45	208.14	209.84	211.54
2.2	213.25	214.97	216.70	218.44	220.19	221.95	223.72	225.50	227.28	229.08	230.88	232.69	234.52	236.35	238.19	240.04	241.90	243.77	245.65	247.54
2.3	249.43	251.34	253.26	255.18	257.12	259.06	261.02	262.98	264.95	266.94	268.93	270.93	272.95	274.97	277.00	279.04	281.09	283.16	285.23	287.31
2.4	289.40	291.50	293.61	295.73	297.86	300.00	302.15	304.31	306.48	308.67	310.86	313.06	315.27	317.49	319.72	321.96	324.22	326.48	328.75	331.04
2.5	333.33	335.63	337.95	340.27	342.61	344.95	347.31	349.68	352.05	354.44	356.84	359.25	361.67	364.10	366.54	368.99	371.46	373.93	376.42	378.91
2.6	381.42	383.93	386.46	389.00	391.55	394.11	396.68	399.27	401.86	404.47	407.08	409.71	412.35	415.00	417.66	420.33	423.02	425.71	428.42	431.13
2.7	433.86	436.60	439.36	442.12	444.89	447.68	450.48	453.29	456.11	458.94	461.79	464.64	467.51	470.39	473.28	476.18	479.10	482.03	484.97	487.92
2.8	490.88	493.86	496.84	499.84	502.85	505.88	508.91	511.96	515.02	518.09	521.18	524.27	527.38	530.50	533.64	536.78	539.94	543.11	546.30	549.49
2.9	552.70	555.92	559.16	562.41	565.67	568.94	572.22	575.52	578.83	582.16	585.50	588.85	592.21	595.58	598.97	602.38	605.79	609.22	612.66	616.12
3.0	619.59	623.07	626.57	630.08	633.60	637.13	640.68	644.25	647.82	651.41	655.02	658.64	662.27	665.91	669.57	673.25	676.93	680.64	684.35	688.08
3.1	691.83	695.58	699.36	703.14	706.94	710.76	714.59	718.43	722.29	726.16	730.05	733.95	737.87	741.80	745.75	749.71	753.69	757.68	761.69	765.71
3.2	769.74	773.80	777.86	781.95	786.04	790.15	794.28	798.43	802.59	806.76	810.95	815.16	819.38	823.61	827.87	832.14	836.42	840.72	845.04	849.37
3.3	853.72	858.09	862.47	866.87	871.28	875.71														

phases at pressure close to 36 atm are also based on experiments.[33] The dashed lines denote the lines of thermoosmotic equilibrium, i.e., equilibrium along capillaries or porous partitions, through which superfluid helium (He^4) passes without resistance and He^3 passes many times more slowly. In this case there is rapidly established a dynamic equilibrium corresponding to the presence of temperature and concentration gradients whose distribution is described by the dashed lines. It should be noted that at increased pressures the $T-\nu$ diagram of He^3 in He^4 is quite complicated, has not yet been finally established experimentally,[34-36] and will not be considered here.

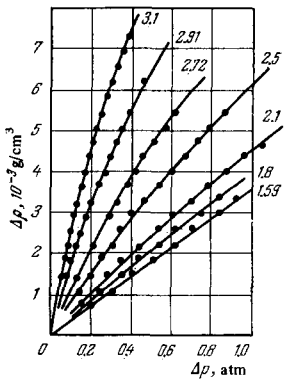

FIG. 4. Compressibility curves of liquid He^3. The numbers on the curve denote T in degrees K.

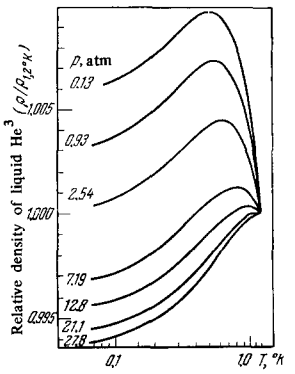

FIG. 5. Relative density of liquid He^3 (ρ/ρ 1.2°K).

2. REFRACTIVE INDEX AND DIELECTRIC CONSTANT

On the basis of a number of measurements[37-40] it can be concluded that both for He^4 and He^3, in either the liquid or gaseous state, the following formula is satisfied with sufficient accuracy (within less than 1%) for the molar polarization

$$\frac{3}{4\pi}\frac{n^2-1}{n^2+2}\frac{M}{\rho}=A \qquad (1)$$

and accordingly for the dielectric constant

$$\frac{3}{4\pi}\frac{\varepsilon-1}{\varepsilon+2}\frac{M}{\rho}=A; \qquad (2)$$

here n is the refractive index, ε the dielectric constant of helium, M the molecular weight, and ρ the density of the helium. For these equations, the constant is A = 0.123 cm^3/mole.

3. COMPRESSIBILITY AND THERMAL EXPANSION

Using the foregoing formulas, we can measure the compressibility of He^3 by observing the shift of the interference fringes. Thus, for example, for the compressibility of gaseous He^3 at temperatures from 1.6° to 3.4°K and densities up to 0.04 g/cm^3, the following relation was obtained:[37]

$$\frac{p}{\rho}=27{,}35T-2.3\cdot10^3\rho+1.8\cdot10^4\rho^2, \qquad (3)$$

where p is the pressure in atmospheres, ρ the density of gaseous He^3 in g/cm^3, and T the temperature in degrees Kelvin.

The curves shown in Fig. 4 were obtained for the compressibility of liquid He^3 by the same method.[37] Figure 5 shows the curves of relative variation of the density of liquid He^3 with increasing temperature, measured[40] on the basis of formula (2) from the change of frequency (15 MHz) of a resonant circuit with a helium-filled capacitor.

There are also direct measurements[41] of the molar volumes and coefficients of thermal expansion of liquid He^3 obtained by filling the measuring volume with

Table II. Molar volumes and coefficients of thermal expansion of liquid He^3 at saturated-vapor pressure

T_{62}	V_m, cm^3/mole	$\alpha_3\times10^3$	T_{62}	V_m, cm^3/mole	$\alpha_3\times10^3$	T_{62}	V_m, cm^3/mole	$\alpha_3\times10^3$
0.00	36.8346	−0.00	0.46	36.7128	−1.98	1.45	37.4326	44.99
0.02	36.8337	−2.31	0.48	36.7117	−1.04	1.50	37.5201	48.46
0.04	36.8312	−4.28	0.50	36.7113	−0.09	1.55	37.6144	51.87
0.06	36.8275	−5.92	0.52	36.7116	+0.86	1.60	37.7151	55.65
0.08	36.8226	−7.27	0.54	36.7126	1.81	1.65	37.8219	61.00
0.10	36.8168	−8.34	0.56	36.7143	2,75	1.70	37.9339	65.60
0.12	36.8104	−9.16	0.60	36.7197	4,60	—	—	—
0.14	36.8034	−9.76	0.65	36.7302	6,82	1.80	38.201	75.10
0.16	36.7961	−10.15	0.70	36.7447	8.94	1.90	38.507	84.69
0.18	36.7885	−10.35	0.75	36.7630	10.96	2.00	38.854	94.57
0.20	36.7809	−10.38	0.80	36.7849	12.89	2.10	39.243	104.83
0.22	36.7733	−10.26	0.85	36.8103	14.76	2.20	39.680	116.84
0.24	36.7658	−10.01	0.90	36.8392	16.60	2.30	40.173	130.50
0.26	36.7586	−9.63	0.95	36.8715	18.46	2.40	40.734	146.93
0.28	36.7517	−9.15	1.00	36.9073	20.37	2.50	41.377	167.06
0.30	36.7451	−8.58	1.05	36.9467	22.38	2.60	42.124	191.88
0.32	36.7391	−7.93	1.10	36.9901	24.53	2.70	43.033	222.34
0.34	36.7335	−7.21	1.15	37.0376	26.85	2.80	44.049	259.33
0.36	36.7285	−6.43	1.20	37.0897	29.37	2.90	45.304	303.50
0.38	36.7241	−5.60	1.25	37.1467	32.11	3.00	46.818	355.24
0.40	36.7203	−4.73	1.30	37.2091	35.07	3.10	48.652	414.53
0.42	36.7171	−3.84	1.35	37.2773	38.22	3.20	50.876	480.86
0.44	36.7146	−2.92	1.40	37.3517	41.55			

Table III. Molar volumes and coefficients of compressibility of solid He^3 and He^4

Pressure bars	Observed relative change of volume $-\Delta V/V_{2000}$		Molar volume cm^3/mole		Compressibility coefficient $\beta_T = -\frac{1}{V}\left(\frac{\partial V}{\partial P}\right)_T$, 10^{-5} bar^{-1}	
	He^4	He^3	He^4	He^3	He^4	He^3
Melting	—	—	17.00	17.56	102	104
1 000	—	—	12.25	12.86	17.6	19.7
2 000	0	0	10.72	11.07	9.72	10.13
3 000	0.074	0.082	9.93	10.16	7.05	7.12
4 000	0.125	0.133	9.38	9.60	5.60	5.65
5 000	0.164	0.173	8.96	9.15	4.67	4.68
6 000	0.199	0.206	8.59	8.79	3.94	4.00
8 000	0.253	0.258	8.01	8.21	3.01	3.07
10 000	0.293	0.299	7.58	7.76	2.44	2.47
12 000	0.327	0.331	7.21	7.41	2.01	2.08
14 000	0.353	0.357	6.94	7.12	1.75	1.80
16 000	0.373	0.380	6.72	6.86	1.55	1.57
18 000	0.391	0.398	6.53	6.66	1.40	1.41
20 000	0.406	0.415	6.37	6.48	1.27	1.27

He^3. The data obtained in these measurements at saturated-vapor pressure are given in Table II.

Table III lists data[42] on the pressure dependence of the molar volumes and the compressibility coefficients of solid He^3 and He^4 at T = 4.2°K and to pressures up to 20,000 bar (1 bar ≈ 1 atm).

4. SURFACE TENSION

Owing to the weak interaction between the atoms of liquid helium, its surface tension is very small. The surface tension of He^3 at the lowest temperatures is only $\alpha = 0.152$ dyne/cm, which is 500 times smaller than in water, almost 100 times smaller than in liquid nitrogen, 20 times smaller than in hydrogen, and 2.3 times smaller than in liquid He^4. It is curious that the plots of α/α_0 against T/T_c, where α_0 is the value of the surface tension at T = 0°K and T_c is the critical temperature, are the same for He^3 and He^4. Figure 6 shows a plot of α against T for He^3, corresponding to the data of Zinov'eva,[43] and for He^4 in accordance with the data of Allen and Misener.[44]

5. ADSORPTION

The adsorption of He^3 by activated charcoal was measured by Hoffman, Edeskuty, and Hammel.[45] According to their data, the heat of sorption of He^3 is 190 J/mole at 3°K and 180 J/mole at 2.45°K. The amount of sorbed He^3 at pressures ranging from 0.1 to 0.9 of the saturated-vapor pressure at a given temperature (2.45° and 3°K) remains practically unchanged and amounts to 0.43 cm^3_0/m^2. At lower pressures, the amounts of sorbed He^3 decreased sharply.

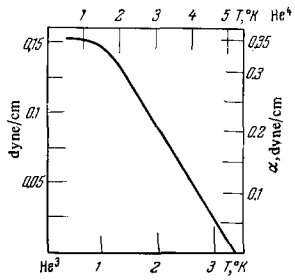

FIG. 6. Surface tension of He^3 and He^4.

Brewer, Symonds, and Thomson[46] measured the adsorption of He^3 by a glass filter in which the pores were capillaries measuring approximately 30 Å. According to their data, 0.5 cm^3_0/m^2 is sorbed at T = 3°K and $p/p_{sat} = 0.1$. The amount of sorbed He^3 increases almost linearly with increasing pressure and reaches 1.1 cm^3_0/m^2 at $p/p_{sat} = 0.9$. Here cm^3_0 is the volume of the gas at 1 atm pressure and t = 0°C, p/p_{sat} is the ratio of the pressure of the gas to the pressure of the saturated vapor at the given temperature, and m^2 is a square meter of active surface of the sorbant. At T = 0.625°K, the volume of the adsorbed gas increases almost linearly from 0.8 cm^3_0/m^2 at $p/p_{sat} = 0.1$ to 1.2 cm^2_0/m^2 at $p/p_{sat} = 0.5$, and the sorption does not increase any more, up to saturation pressure. It should be noted that under analogous conditions the amount of sorbed He^4 is larger by a factor 1.2–1.3.

In the sorption of He^3–He^4 mixtures, large enrichment of the sorbed He^4 phase was observed.[47] Thus, at an He^3 concentration in the adsorbed phase from 0.0015 to 0.005, the concentration of the vapor phase exceeds the concentration of the adsorbed phase by 23 times at T = 1.6°K, by 16 times at T = 1.8°K, by 13 times at T = 2°K, and by 10 times at T = 2.3°K.

6. SOUND IN HELIUM, ZERO SOUND

The velocity of sound in He^3 was measured by a number of workers. The temperature dependence of the sound velocity in liquid and solid He^3 and in solutions of He^3 in He^4, plotted from the experimental data,[48-51] is shown in Fig. 7. The curve for liquid He^4 was plotted at saturated-vapor pressure, while the curves for 25% and 75% solutions He^3 in He^4 were obtained at atmospheric pressure. On the curves for He^4 and for the 25% solution one can see the characteristic change of the curve on approaching the λ point. The damping of sound in pure He^4 has a maximum[52] at temperatures at which the mean free path of the phonons becomes comparable with the wavelength of the sound. Thus, at 14 MHz frequency, the maximum of the damping coefficient K = 3 cm^{-1} ($A = A_0 \exp[-kx]$) lies in the region 0.9°K. In solutions of He^3 in He^4 with concentration $\nu = 0.012$, the coefficient decreases to K = 1 cm^{-1}, and at $\nu = 0.052$ it decreases to K = 0.5 cm^{-1}.

The lower curve at temperatures higher than 0.5°K corresponds to saturated-vapor pressure, and below 0.2°K to a pressure of 0.32 atm. As seen from the figure, a sharp change in the speed of sound is observed at T ~ 0.01–0.02°K. This change is accompanied[51] by considerable damping; thus, for example, at a sound

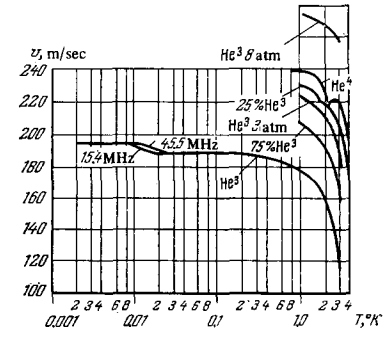

FIG. 7. Temperature dependence of speed of sound in liquid He^3 and in solutions of He^3 in He^4.

frequency 45.5 MHz, the damping coefficient changes from $K = 5\ cm^{-1}$ at $T = 0.2°K$ to a value $K = 200\ cm^{-1}$ at $T = 0.03°K$, and then, after $K = 200\ cm^{-1}$ at $T = 0.012°K$, it decreases rapidly with decreasing temperature, again reaching values lower than $K = 10\ cm^{-1}$.

For a lower frequency, 15.4 MHz, the maximum damping is observed at $T = 0.01°K$, where $K = 90\ cm^{-1}$. This phenomenon, which is unique to He^3 and is connected with the quantum character of sound at very low temperatures, was theoretically predicted by Landau,[53] called by him zero sound, and first observed by Keen, Matthews, and Wilks.[54] Figure 7 shows also plots of the speed of sound in He^3 against the temperature at pressures 2 and 8 atm.[49]

Figure 8 shows a plot of the speed of sound against the pressure in solid He^3 and He^4 for different crystal lattices—cubic (bcc) and hexagonal (hcp). The curves are based on experimental data,[50] but the authors themselves note that the speed of sound in solid helium should depend on the direction. This is manifest in the experiments by the fact that the values of the speed under the same conditions vary as much as 12% from experiment to experiment. The damping of sound in solid He^3 was of the order $K = 0.3-0.7\ cm^{-1}$. Data on the speed of sound in gaseous He^3 are available[55] only in a very narrow region. At $T = 4.2°K$ the speed of sound in He^3 increases from 163 m/sec at $p = 3.58$ atm to 194 m/sec at 4.81 atm. At $T = 3.315°K$ and $p = 3.99$ atm, the speed of sound is 208 m/sec. The measurements were made at 14 MHz. It is seen from these data that the speed of sound in gaseous helium is somewhat larger than the speed of sound in liquid He^3.

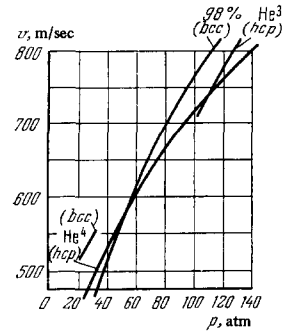

FIG. 8. Pressure dependence of the speed of sound in solid He^3 and He^4 at a temperature close to the melting temperature.

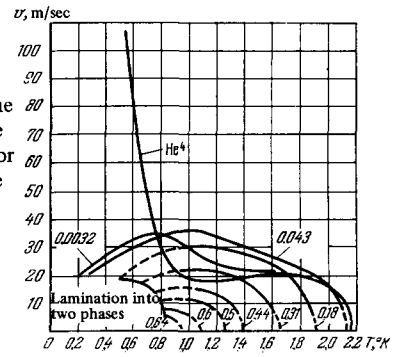

FIG. 9. Dependence of the speed of second sound on the temperature at saturated-vapor pressure. The numbers on the curves denote the molar concentration of He^3 in a liquid solution of He^3 in He^4.

7. SECOND SOUND

Thermal oscillations in liquid He^3 propagate as ordinary rapidly damped thermal waves. However, solutions of He^3 in He^4 have a broad region of superfluid phase (see Fig. 3), in which the thermal oscillations propagate in the form of weakly damped waves of second sound. To be sure, near the λ line, particularly for solutions of large concentration, the damping of second sound is quite appreciable. A plot of the speed of second sound against temperature, plotted for several concentrations on the basis of experimental data[56] at saturated-vapor pressure, is shown in Fig. 9. For comparison, a plot of the speed of second sound against the temperature[57] is shown for pure He^4.

8. SPECIFIC HEAT

The specific heat of liquid He^3 at saturated-vapor pressure[58-60] and at $p = 29$ atm,[59] and also the specific heat of solutions of He^3 and He^4[61, 62] at saturated-vapor pressure with molar He^3 concentrations equal to 0.05, 0.094, 0.15, 0.29, and 0.48, are shown in Fig. 10. For comparison we show a plot of the specific heat of He^4 against the temperature at saturated-vapor pressure.[63] The curves for $\nu = 0.29$ and $\nu = 0.48$ at low temperatures terminate at temperatures corresponding to the start of the stratification into two liquid phases.

At very low temperatures and at He^3 concentration in liquid He^4 equal to 0.05 (lower curve of Fig. 10), the specific heat of the solution coincides with the specific heat of an ideal Fermi gas consisting of He^3 atoms, but

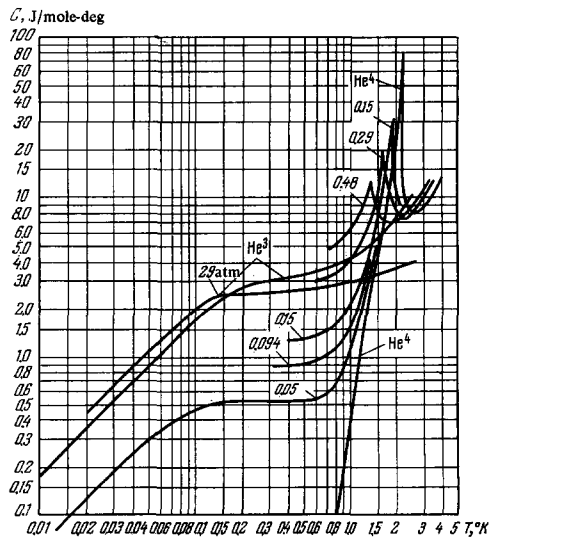

FIG. 10. Specific heat of He^3, He^4, and of solutions of He^3 in He^4.

with an effective mass larger by 2.4 times.

There are measurements[64] of the specific heat of He^3 and He^4 at constant volume C_V with density of approximately 0.99 of critical in the direct vicinity of the critical point. The results of the measurements are given in the following form:

for He^3: $0 < T_c - T < 0.1$,
$$\frac{C_v}{R} = -0.37 \ln\left(\frac{T_c - T}{T_c}\right) + 1.7, \quad (4)$$
$$0 < T - T_c < 0.01, \quad \frac{C_v}{R} = -0.37 \ln\left(\frac{T - T_c}{T_c}\right) - 0.5, \quad (5)$$
for He^4: $0 < T_c - T < 0.1$,
$$\frac{C_v}{R} = -0.62 \ln\left(\frac{T_c - T}{T_c}\right) + 2.0, \quad (6)$$
$$0 < T - T_c < 0.01, \quad \frac{C_v}{R} = -0.62 \ln\left(\frac{T - T_c}{T_c}\right) - 1.6, \quad (7)$$

where $R = 8.31$ J/mole-deg, and T_c is the critical temperature. Figure 11 shows a general form[65] of the

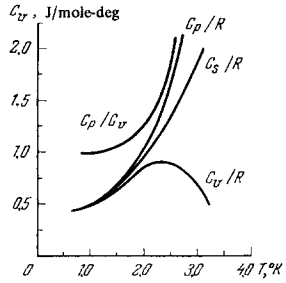

FIG. 11. Specific heat C_V, C_S, and C_p of liquid He^3.

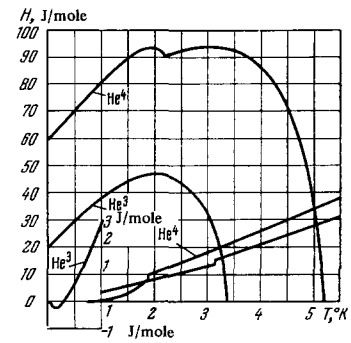

FIG. 12. Heat of evaporation and melting of He^3 and He^4.

temperature dependence of the specific heat of liquid He^3 at constant volume C_V, along the evaporation curve C_S, and at constant pressure C_p. Measurements[66] have shown that the specific heats of He^3 and He^4, which form a monatomic layer covering the sorbed surface almost completely (0.74 for He^3 and 0.8 for He^4), from 0.25° to 4°K, are proportional to the square of the temperature. The Debye temperature characteristic of the two-dimensional model is equal to 28°K for He^3 and 31°K for He^4. The specific heat of solid He^3 at temperatures from 6.3 to 14°K and at molar values from 24.4 to 12.57 cm^3/mole can be expressed, according to the measurements of [67, 68], in the form

$$C_v = AT + 1.93 \cdot 10^3 \frac{T^3}{\Theta^3} \text{ (J/mole-deg)}. \quad (8)$$

The dependence of the Debye temperature Θ on the molar volume v, for both hexagonal crystals (hcp) and cubic crystals (bcc), is given by the formula

$$\frac{d \ln \Theta}{d \ln v} = -2{,}5. \quad (9)$$

At the transition point, at v = 20 cm^3/mole, $\Theta = 35°K$ for hexagonal crystals and Θ = 29°K for cubic crystals.

The specific heat of solid hexagonal crystals of He^4 was also determined[69] from formulas (8) and (9). The values of the Debye temperatures coincide in this case with the values of Θ for cubic He^3 crystals. In place of the term AT in formula (8), the authors propose also a correction proportional to $T^{-1} \exp(-\Phi/T)$, indicating that the value of Φ coincides with the value obtained from the activation energy in the self-diffusion process. It follows from the experimental data,[67] however, that the correction to the Debye term in formula (8) has an irregular character, changes from 0 to 0.009 J/mole, and is connected with the imperfection of the crystals due to the impurities or vacancies in this location.

9. HEATS OF PHASE TRANSITIONS

The heats of evaporation and melting of He^3 and He^4 are usually calculated with the aid of the thermodynamic equation

$$H = T(v_1 - v_2)\frac{dp}{dT}, \quad (10)$$

where H is the heat of the transition, T the absolute temperature, v_1 the volume of the less dense phase, v_2 that of the denser phase, and dp/dT the derivative of the pressure with respect to temperature along the phase-equilibrium curve.

The upper curves of Fig. 12 show the temperature dependence of the heats of evaporation of He^3 and He^4, obtained from formula (10) on the basis of experimental data on the molar volumes and vapor-tension curves.[70-72] The available experimental data[73-75] obtained by direct measurement of the heat of evaporation agree with the data obtained with formula (10).

The lower curves of Fig. 12 represent the heat of melting of He^3 and He^4, also calculated from formula (10) on the basis of experimental data on the molar volumes and the (p-T) melting curves.[76-79] For He^4 in the interval 1.45-1.78°K, there is a small region of existence of a body-centered cubic (bcc) phase (see Fig. 2). According to estimates by formula (10), the heat of transition from the hexagonal (hcp) phase into the less dense cubic (bcc) phase, amounts to 0.4 J/mole at T = 1.7°K.

At 0.77°K and p = 25.0 atm, a minimum is observed[80] on the melting curve of He^4, and therefore the heat of melting vanishes at this point, while at temperatures lower than the minimum crystallization of He^4 by compression leads not to a release of heat but to absorption of heat. To be sure, this heat is only 3.5×10^{-4} J/mole at T = 0.7°K, and is even smaller at other temperatures.

A transition of He^3 from the hexagonal to the cubic phase was observed[14] at 3.15°K. The heat of the transition, calculated from formula (10), is approximately 1.8 J/mole at 3.15°K and only 0.5 J/mole at 2°K. As seen from Fig. 12, the heat of melting of the hexagonal phase is somewhat higher than that of the cubic phase. On the lower left of Fig. 12 is shown, magnified ten times, the heat of melting of He^3 at temperatures below 1°K. Special notice should be taken here of the fact that below 0.32°K the heat is absorbed rather than released upon crystallization, and the heat of the transition is approximately 0.25 J/mole at 0.15°K, making it possible to use the process of adiabatic crystallization to obtain very low temperatures.

10. ENTROPY DIAGRAM OF He^3

The entropy diagram for He^3 was plotted[59] by using the formula

$$S = \int_0^T \frac{c\,dt}{T}, \quad (11)$$

and extrapolating linearly the temperature dependence of the specific heat to 0°K, or else by calculating the entropy of gaseous He^3 at 1.5°K, subtracting from it the entropy of the transition from the liquid phase to the gas phase using the heat of transition measured at the same temperature,[81] and then calculating the entropy for other temperatures from formula (11).

It is possible, however, to use the fact that at T = 0.32°K the melting curve of He^3 has a minimum and the entropies of the solid and liquid helium should be equal at this point. Taking into account, further, the fact that the Debye temperature of solid helium is much higher than 0.32°K, and therefore the contribution of the phonon part to the entropy is very small, and that magnetic ordering in solid He^3 begins, in the extreme case, below several hundredths of a degree (as follows from Anufriev's experiments[82] on adiabatic crystallization), it can be assumed that at this point the entropy of the liquid and solid He^3 differ very little from R ln 2. The value of the entropy for other states can be obtained from the available data on the specific heat of solid and liquid He^3, the heats of transition, and also the difference of the entropies upon compression.[83] The entropy diagram obtained in this manner is shown in Fig. 13. The curve which is lower up to 1°K and higher above 1°K corresponds to the entropy of the liquid in equilibrium with the saturated vapor. The curves marked 1, 5, 10, 30, and 50 atm correspond to values of the entropy of the liquid at pressures 1, 5, 10, 30, and 50 atm. The lower curve of this series, at temperatures higher than 0.32°K, corresponds to the entropy of the liquid in equilibrium with the solid He^3, and below 0.32°K to the entropy of the liquid at a pressure p = 29 atm. The vertical line at 3.15°K corresponds to the triple point, where the liquid and hexagonal and cubic phases of He^3 coexist. The lines marked (bcc) and (hcp) correspond to the entropies of the cubic and hexagonal crystals in equilibrium with each other. The upper line of this part of the diagram corresponds to the entropy of the cubic crystals in equilibrium with the liquid. The place where the entropy of the solid He^3 drops sharply in the region of low temperatures is set arbitrarily, since there are no reliable experimental data concerning the temperature of the start of spin ordering in solid He^3.

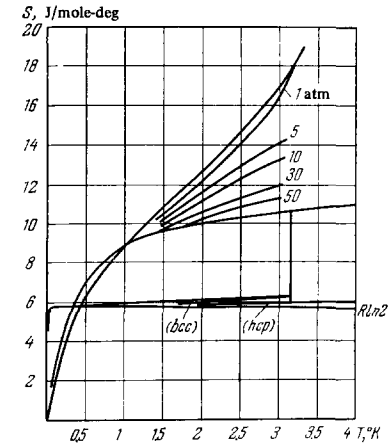

FIG. 13. Entropy diagram of He^3.

11. MAGNETIC PROPERTIES

As already mentioned, the He^3 atom has spin ½ and a magnetic moment $\mu = 1.07 \times 10^{-23}$ erg/G, or 0.7618 μ_p (where μ_p is the magnetic moment of the proton). Therefore the magnetic susceptibility of He^3 gas in the region where it is possible to use not quantum but classical statistics, is equal to

$$\chi = \frac{n\mu^2}{3kT}, \qquad (12)$$

where n is the number of atoms of He^3 per cm^3 and k is Boltzmann's constant. At 2°K and $n = 1.6 \times 10^{22}$ cm^{-3} (corresponding to the density of liquid helium) we have $\chi \approx 2.2 \times 10^{-9}$, i.e., its absolute magnitude is almost impossible to measure. However, many measurements were made of the temperature dependence of χ with the aid of nuclear-resonance and spin-echo technique. Figure 14 shows the results of measurements by Beal and Hatton,[84] performed on liquid He^3 at different pressures.

At temperatures higher than 2°K, liquid He^3 satisfies the Curie law, i.e.,

$$\chi T = B, \qquad (13)$$

where B is the Curie constant. At lower temperatures, the ordering of the magnetic moments connected with their interaction sets in. At very low temperatures χ does not depend on T.

If we plot $\chi T/B$ as a function of $\tau = T/T_F$ where $T_F = 3B/2\chi_0$ is the Fermi temperature and χ_0 is the value to which χ tends when $T \to 0$, then all the experimental data fit one curve (Fig. 14). Then T_F depends on the pressure in the following manner:

P, atm:	0.7	3.6	11	18	27
T_F, °K:	0.55	0.5	0.41	0.36	0.32.

Measurements[85] of the temperature dependence of the magnetic susceptibility of solutions of He^3 and He^4 in the molar-concentration interval from 0.14 to 1.00 have shown that the Curie law is satisfied accurate to 1% at temperatures from 1.9 to 2.9°K. The authors propose that the satisfaction of the curie law is due to the compensation of the deviations caused by effects connected with exchange interaction between the nuclear moments and with the interaction that leads to satisfaction of the Pauli principle. It can be proposed that in this case the absolute value of the magnetic susceptibility is determined by formula (12).

Measurements[62, 86] of the magnetic susceptibility of solutions of He^3 in liquid He^4 in the temperature interval from 0.05° to 0.7° for $\nu = 0.5$ and from 0.04° to 0.26°K for $\nu = 0.013$ have shown that χ is very close to the magnetic susceptibility of an ideal Fermi gas whose degeneracy temperature coincides with the values of T_F determined from measurements of the specific heat. (χ can be calculated with the aid of the tables of [87].)

Measurements of the magnetic properties of solid He^3 have shown[88, 89] that in the case when the experiments are carried out under equilibrium conditions the

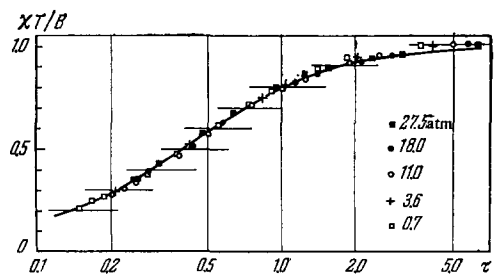

FIG. 14. Dependence of χ T/B on $\tau = T/T_F$.

magnetic susceptibility of solid He^3 obeys the Curie law, at least when T exceeds 0.06°K. Experiments with He^3 are made complicated by the very long times, on the order of tens of minutes, necessary to establish thermal equilibrium between the system of nuclear spins and the crystal lattice. In this case even small (0.05%) admixtures of He^4 greatly affect the measurement results.

Measurements have been reported[90] of the nuclear susceptibility of He^3 sorbed on glass. The susceptibility of the first layer obeys the Curie law in the temperature interval from 0.3° to 2°K, and the susceptibility of the second layer is determined by the formula $\chi = B/(T + \Theta)$ with a Curie temperature $\Theta = 0.04°K$.

12. RELAXATION TIME

Since the magnetic susceptibility of He^3 is very low and all the reported measurements have been performed by ac nuclear resonance methods, a very important role is played by the time t_1 of establishment of thermal equilibrium between the system of interacting nuclear spins and the liquid or solid helium as a whole, and also the time t_2 of establishment of equilibrium within the spin system. It is clear from the very definition that t_1 is larger than or equal to t_2.

The data concerning t_1 in liquid He^3 are subject to great scatter. This is connected with the fact that any paramagnetic impurity located on the walls of the vessel with the liquid He^3, or else suspended in the helium itself, leads to a noticeable decrease of t_1. The longest relaxation times t_1 were observed in the experiments of Romer,[91] where regardless of the magnitude of the magnetic field, from 1.5 to 12 kG, t_1 varied monotonically from 300 sec at 0.75°K to 400 sec at 2°K and 600 sec at 3°K. These relaxation times were smaller by a factor of about $1\frac{1}{2}$ than those calculated on the basis of the Torrey formula[92]

$$\frac{1}{t_1} = \frac{2\pi\gamma^4\hbar^2 N}{5aD}, \qquad (14)$$

where γ is the gyromagnetic ratio, a the atomic diameter ($a \approx 2.7$ Å), N the number of He^3 atoms per cm^3, and D the self-diffusion coefficient. Formula (14) is valid under the condition $\omega_0\tau_0 \ll 1$, where ω_0 is the frequency of the Larmor precession, and the correlation time is $\tau_c = a^2/6D = 3 \times 10^{-12}$ sec. In this case $t_2 \approx t_1$.

It follows from (14) that the relaxation time t_1 can be very large at temperatures much lower than 1°K, where $\sim T^{-2}$.

According to the measurements of Garwin and Reich,[93] the relaxation times t_1 in solutions of He^3 in He^4 reach thousands of seconds. In their experiments with pure He^3, however, the times t_1 were much shorter than those obtained by Romer;[91] it can therefore be assumed that, owing to the presence of magnetic impurities in the suspended state or on the walls, the values of the relaxation obtained were too low in solutions as well.

Measurement of the relaxation time t_1 in solid He^3 crystals is quite difficult, since the condition $\omega_0\tau_0 \ll 1$ is not satisfied here and t_1 increases with increasing frequency at which the measurements are performed. In addition, the presence of Zeeman energy in the nuclear-spin system greatly complicates the processes of establishment of thermal equilibrium, producing as it were three weakly interacting heat baths[94] with exchange and Zeeman nuclear-spin energies and with the lattice-vibration energy. The establishment of equilibrium is very strongly influenced by small impurities of He^4 and by lattice inhomogeneities. Measurements[95] under identical conditions give for t_1 in the cubic (bcc) phase of He^3 values which are approximately one hundredth those in the hexagonal phase.

The relaxation times in solid He^3 change from fractions of a second at T = 1°K to thousands of seconds at lower temperatures and higher densities. However, there are no fully reliable data on the relaxation time in pure He^3 crystals.

13. SELF-DIFFUSION IN He^3

The spin-echo technique makes it possible to measure the coefficient self-diffusion in He^3. If a signal produced by nuclear-spin precession is observed in an inhomogeneous magnetic field after a train of oscillations at the resonant frequency caused the spins to rotate through 90°, then the signal attenuates rapidly, owing to the different precession frequencies in different magnetic fields. If one more train of oscillations is now applied, turning all spins through 180°, then they begin to precess in the opposite direction, and were there no diffusion, they would all be gathered after a certain time in the position they occupied immediately after the 90° pulse, i.e., a signal of the same amplitude, called spin echo, would be observed. However, owing to self-diffusion, the spins are shifted, then are inaccurately phased, and therefore the amplitude of the echo signal decreases. The ratio of the amplitude of the echo signal to the amplitude of the first signal is

$$\frac{A_2}{A_1} = e^{-t/T_2} e^{-\gamma^2 g^2 D t^3/12}, \qquad (15)$$

where t is the time between the 90° train and the echo, T_2 is the time of exchange relaxation, γ is the gyromagnetic ratio ($\gamma = \omega_0/H_0 = 2 \times 10^4$ rad/sec-G), $g = \partial H/\partial x$ is the gradient of the magnetic field (in G/cm), and D is the self-diffusion coefficient (in cm^2/sec).

Measurements made by this method[93] on liquid He^3 in the temperature interval from 1° to 4°K yield

$$D \text{ cm}^2/\text{sec} = 5.9 \cdot 10^{-5} \ln\left(\frac{0.16}{\rho}\right) e^{T/2.8}, \qquad (16)$$

where ρ is the density of the He^3 and T is its temperature in degrees Kelvin.

At temperatures below 0.03–0.05°K, the coefficient of self-diffusion in liquid He^3 is inversely proportional to the square of the temperature:

$$D = \frac{A}{T^2}. \qquad (17)$$

The value of A changes with pressure[95] from $A = 1.5 \times 10^{-6}$ at 0.3 atm to $A = 1.2 \times 10^{-6}$ at 5 atm. and $A = 2 \times 10^{-7}$ cm^2 deg/sec at 27 atm.

It should be noted that measurements of the coefficient of self-diffusion in liquid He^3 are subject to certain doubts, since a dependence of D on the dimensions of the vessel is observed,[96] although it should not occur in principle. When the diameter of the pyrex glass vessel is increased from 2.5 to 10 mm, the self-diffu-

sion coefficient D at saturated-vapor pressure and a temperature 1–3°K increased[96] by approximately 30%.

The self-diffusion coefficient in solid He^3 was measured by Reich.[97] It turned out that the diffusion process has in this case a thermal-activation character and is described in the cubic (bcc) phase by the equation

$$D = D_0 e^{-T_0/T}, \tag{18}$$

where $D_0 = 3.3 \times 10^{-5}$ cm^2/sec independently of the density, and T_0 is the melting temperature of He^3 at the corresponding density. Thus, $T_0 = 13.7°K$ at an He^3 density $\rho = 0.156$ g/cm³.

In the hexagonal (hcp) phase of He^3, the activation energy for diffusion is approximately double and corresponds to $T_0 = 38°K$.

14. DIFFUSION AND THERMAL CONDUCTIVITY IN SOLUTIONS OF He^3 IN He^4

The diffusion of He^3 in liquid He^4 at temperatures above the λ point is a process similar to diffusion in ordinary liquids. According to measurements by Careri et al.[98]

$$D = (4 \pm 2) \cdot 10^{-5} \text{ cm}^2/\text{sec}. \tag{19}$$

Below the λ point, He^3 takes part in the motion of the normal part, therefore very rapid transport of He^3 is possible, with simultaneous motion of the He^4 in the form of the superfluid part. This produces, besides the difference in the concentrations also a temperature difference, i.e., thermoosmosis is observed. If a constant heat flux is produced in the solution, then a stationary state is established, in which the following relation will hold between the He^3 concentration gradient and the temperature in the case of weak solutions[99]

$$R\nabla(\nu T) = -S\nabla T, \tag{20}$$

where R is the gas constant, ν the molar concentration of He^3 in the solution, and S the entropy per mole of pure He^4.

In this case the heat flux is

$$Q = -\left[\frac{\rho S^2}{MR\nu}\left(\frac{\rho_n}{\rho_{n0}}\right)^2 D + \varkappa\right]\nabla T = -\varkappa_{\text{eff}}\nabla T, \tag{21}$$

where ρ is the density of the solution, M the molecular weight of He^4, $\rho_{n,0}$ the part of the normal density (ρ_n) of the solution due to the rotons and phonons, D the diffusion coefficient, κ the thermal conductivity coefficient, and κ_{eff} the coefficient of effective thermal conductivity.

The first term in this formula corresponds to the heat transfer due to the motion of elementary excitations as a whole (motion of the normal part of liquid helium), and the second, with κ, corresponds to heat transfer, analogous to the usual thermal conductivity, i.e., due to diffusion of thermal excitations.

As seen from (21), the coefficients of thermal conductivity κ and of diffusion D in solutions are organically related and can be determined separately only if one of them is much larger than the other. Experiments of this kind were performed by Ptukha[101] and made it possible to determine D at temperatures above 1.3°K and κ at temperatures below 1.3°K. According to Ptukha's measurements, at concentrations

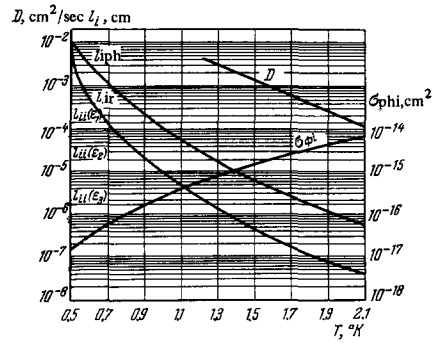

FIG. 15. Temperature dependence of the mean free path of He^3 atoms dissolved in liquid He^4, upon scattering by phonons (l_{iph}), rotons (l_{ir}) and by each other at molar concentrations $\nu = 1.39 \times 10^{-4}$ ($l_{ii}(\epsilon_1)$), 1.32×10^{-3} ($l_{ii}(\epsilon_2)$), and 1.36×10^{-2} ($l_{ii}(\epsilon_3)$), and also the cross sections for scattering of phonons by He^3 atoms (σ_{phi}) and of the diffusion coefficient D of He^3 in solution. The designations $l_{ii}(\epsilon_{1,2,3})$ on the figure are placed exactly over the corresponding lines.

$\nu = 1.39 \times 10^{-4}$ and 1.32×10^{-3} the diffusion coefficient does not depend on the concentration. Its dependence on the temperature is shown in Fig. 15.

At temperatures below 1°K, the main role in heat transfer is played by the phonons, and the thermal conductivity decreases with increasing concentration. Thus, at T = 0.7°K the thermal conductivity drops from 5×10^{-2} W/cm-deg at $\nu = 1.39 \times 10^{-4}$ to 1.2×10^{-2} at $\nu = 1.32 \times 10^{-3}$ and to 1.3×10^{-3} W/cm-deg at $\nu = 1.36 \times 10^{-2}$. Figure 15 shows also the free path of the thermal excitations and of atoms of He^3 dissolved in He^4, calculated by Ptukha on the basis of the theory of diffusion and thermal conductivity of weak solutions of He^3 in superfluid helium.[100] The diffusion of He^3 in He^4 in a gas with average concentration of approximately 8% He^3 at pressure 15–30 mm Hg. was measured by Bendt.[102] He measured not the diffusion coefficient D directly, but the product $nD\mu$ (g/cm-sec), where n is the number of atoms per cm^3 and $\mu = 2.84 \times 10^{-24}$ g is the reduced mass for collision of He^3 atoms with He^4 atoms. In the temperature interval between 1.74° and 296°K, the value of $nD\mu$ changes from 3.99×10^{-6} to 1.18×10^{-4} g/cm-sec. In the range from 1.7° to 4°K $nD\mu$ can be represented in the form

$$nD\mu = 2.58 \cdot 10^{-6} T^{0.79} \text{ g/cm-sec} \tag{22}$$

and above, up to 300°K, in the form

$$nD\mu = 3.15 \cdot 10^{-6} T^{0.64} \text{ g/cm-sec} \tag{23}$$

15. THERMAL CONDUCTIVITY OF He^3

Figure 16 shows the results of measurements of the thermal conductivity of gaseous He^3 and He^4, made by Fokkensk et al.[103] at pressures on the order of 0.1 mm Hg, and also the data on the measurements of the thermal conductivity of liquid non-superfluid He^4 and liquid He^3 at pressures of approximately 0.6 atm,[104] and measurements at temperatures from 0.9° to 0.06°K at two pressures.[105]

In the upper portion, on the basis of measurements by Bertmann et al.,[106, 107] are plotted the temperature dependences of the thermal conductivities of solid He^3 and He^4 and of crystals with molar concentrations of He^4 equal to 0.013, 0.04, 0.1, and 0.5 at crystal molar

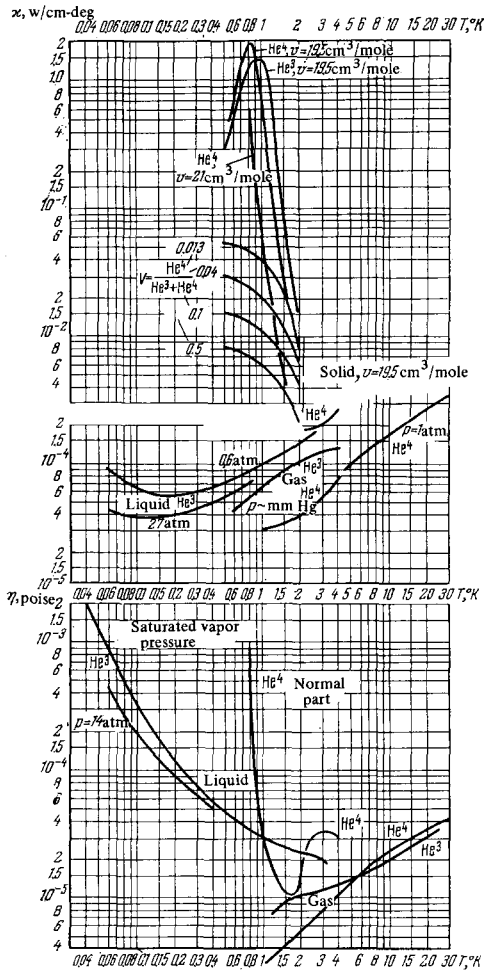

FIG. 16. Thermoconductivity and viscosity of He^3 and He^4.

volumes of 19.5 cm^3/mole, and for He^4—with molar volume 21 cm^3/mole.

It is indicated in the papers of Bertman et al. that the He^3 and He^4 were very pure, but the degree of purity was not determined numerically. At the same time, it is clear from other investigations,[108,109] that the thermal conductivity of solid helium depends strongly not only on the purity but also on the perfection of the crystals. In any case, the thermal conductivity κ of a cylindrical He^4 single crystal of 2.5 mm diameter, grown at 85 atm, can reach 50 W/cm-deg at T = 0.9°K.[108] Therefore a numerical analysis of the thermal-conductivity curves and calculations of the so-called "Umklapp" phenomena and the associated decrease of thermal conductivity at low temperatures can be performed on the basis of the presented data only approximately.

16. THE KAPITZA JUMP

Kapitza[110] observed that at low temperatures, when heat is transferred from a solid to liquid h' lium, a temperature jump occurs on the boundary. The jump consists in the fact that the transfer of heat is in this case connected primarily with transition of phonons, sound quanta, from the solid into the liquid, and the probability of such a process is low. Thus, at a large acoustic-stiffness difference, the fraction of the sound energy passing through the boundary is

$$K = 4\rho_l u_l \cos\vartheta/\rho_s u_s, \tag{24}$$

where ρ_l, u_l and ρ_s, u_s are the density and speed of sound respectively for the liquid and solid, and ϑ is the angle of incidence of the sound on the boundary in the solid. The total energy flux carried by the phonons of the solid into the liquid through a unit surface of the boundary is

$$W_l = \frac{1}{2}\int_0^{\pi/2} \mathcal{E}_{ph} u_s K \cos\vartheta \sin\vartheta \, d\vartheta = \frac{2\rho_l u_l \mathcal{E}_{ph}}{\rho_s}\int_0^{\pi/2} \cos^2\theta \sin\vartheta \, d\vartheta = \frac{2\rho_l u_l \mathcal{E}_{ph}}{3\rho_s}, \tag{25}$$

where $\mathcal{E}_{ph}$ is the average energy of the phonons per cm^3 of the solid. In equilibrium, the same amount of heat will be carried from the liquid into the solid. If the temperature T_1 of the solid is not equal to the temperature T_2 of the liquid, a constant heat flux is produced.

$$W = \frac{2\rho_l u_l}{3\rho_s}[\mathcal{E}_{ph}(T_1) - \mathcal{E}_{ph}(T_2)] = \frac{2\rho_l u_l}{3\rho_s}\frac{\partial \mathcal{E}_{ph}}{\partial t}\Delta T = \frac{2\rho_l u_l c_{ph}\Delta T}{3}, \tag{26}$$

or

$$R = \frac{\Delta T}{W} = \frac{7{,}7\cdot 10^{-4} M\Theta^3}{\rho_l u_l T^3} (\mathrm{cm^2\ deg}\ ; \tag{27}$$

here $c_{ph} = 1944\ T^3/M\Theta^3$ J/g-deg is the phonon part of the specific heat of the a solid whose molecular weight is M and whose Debye temperature is Θ. Substituting in (27) the data for copper (M = 65.54 g/mole and Θ = 339°) and He^3 (ρ_l = 0.08 g/cm^2, $u_l = 1.9\times 10^4$ cm/sec), we get

$$R_3 = 1300/T^3\ \mathrm{cm^2\ deg/W} \tag{28}$$

and for He^4 (ρ_l = 0.145 g/cm^3, $u_l = 2.4\times 10^4$ cm/sec)

$$R_4 = 570/T^3\ \mathrm{cm^2\ deg/W} \tag{29}$$

Inasmuch as solid helium also has an acoustic stiffness which is many times smaller than that of copper, formula (27) can be employed for it, too. In this case for solid He^3 with ρ = 0.13 g/cm^3 and $u = 6\times 10^4$ cm/sec we have

$$R_{3s} = 250/T^3\ \mathrm{cm^2\ deg/W} \tag{30}$$

and for He^4 with ρ = 0.2 g/cm^3 and $u = 6.6\times 10^4$ cm/sec we have

$$R_{4s} = 160/T^3\ \mathrm{cm^2\ deg/W} \tag{31}$$

It is clear that the picture under consideration gives only the general physical idea of the process, and does not take into account the anisotropy of the solid and the presence of transverse waves. This, however, changes the results very little, while more detailed calculations[111,112] give for R values of the same order. At the same time, the experimental results show that the temperature dependence of R, as a rule, differs from T^{-3}, and the absolute values of R depend very strongly on the state of the surface and are smaller by several dozen times than would follow from the estimates given above. Thus, according to the data of Lee and Fairbank we have for He^3 and copper from 0.4° to 2°K $R = 130/T^2$ cm^2 deg/W, while Fairbank and Wilks[113] obtained for He^4 and copper $R = 45/T^2$.

Kuang Wei-yen[114] obtained the relation

$R = 21/T^{2.6}$ cm² deg/W for copper and He^4 from 0.57° to 2°K. Anderson et al.[105] give for He^3 a value $R = 200/T^3$ at temperatures from 0.05° to 0.1°K, and $R \sim 1/T^4$ in the interval 0.1–0.4°K. At increased pressures in liquid helium, only a small change takes place in the heat jump,[114] smaller by several times than follows from formula (27).

For solid He^3, Anderson et al.[115] obtained $R = 60/T^3$ cm² deg/W in the interval 0.07×0.2°K, but from 0.2° to 0.7°K the thermal resistance is inversely proportional to T^4.

It is thus clear at low temperatures (T < 0.1°K), the Kapitza jump is the greatest obstacle to the establishment of equilibrium in the apparatus, and all experiments give a sharp increase of R with decreasing temperature. However, the large difference between the data of different experiments and between the experimental and theoretical estimates indicates that the conditions on the boundary of the solid are far from ideal. A possible cause is the presence on the surface of mechanically finished metals of a strongly deformed amorphous layer[114, 116] of thickness 5×10^{-7}–10^{-6} cm, which leads to an increase of the effective surface and to "acoustic transparency" of the boundary. The resolution of this contradiction should be found in subsequent experiments.

17. VISCOSITY

Figure 16 shows data on the temperature dependence of the viscosity of liquid He^3 [117-119] at saturated-vapor pressure and at p = 14 atm. At temperatures lower than 0.1°K, the dependence of the viscosity of liquid He^3 on the temperature, at saturated-vapor pressure, is close to $\eta = 3.2 \times 10^{-8}/T^2$ poise.

For comparison, we present the data of [117, 120] for the viscosity of liquid He^4 above the λ point and the viscosity of the normal part of superfluid He^4 below the λ point. On the lower right are plots of the temperature dependence of the viscosity of gaseous He^3 and He^4 according to the measurement data of [121, 122], at a pressure of a fraction of a mm Hg. At the critical point, the viscosities of gaseous and liquid helium should be equal. However, viscosity of the gas is independent of the pressure in first approximation, therefore it is not clear from the curves of Fig. 16 how the viscosities of the liquid and gaseous helium can be comparable at the critical point. It is obvious that further experiments are necessary to answer this question.

18. EXPERIMENTS AIMED AT FINDING THE TRANSITION OF LIQUID He^3 INTO THE SUPERFLUID PHASE

Inasmuch as, in analogy with electrons in superconductors, the He^3 atoms are prone to noticeable pair interaction, owing to the presense of nuclear spins, He^3 should become superfluid at very low temperatures.[3] This question is the subject of a large number of papers. In the first experiment[123] in which it was possible to measure the specific heat of liquid He^3 to the very lowest temperatures obtainable and measurable with the aid of cerium-magnesium nitrate (CMN), a maximum of the specific heat is observed at temperatures on the order of 0.055°K as seen from Fig. 17

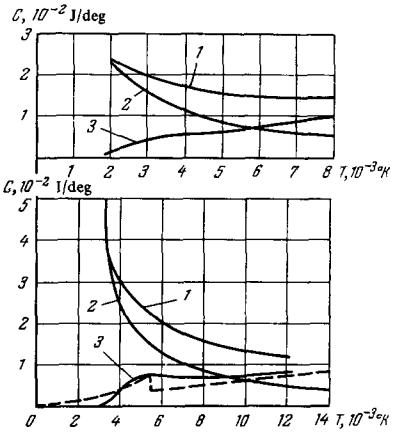

FIG. 17. Specific heat of liquid He^3 and of cerium-magnesium nitrate (CMN) obtained in the experiments of [123] (below) and [124] (above). 1–specific heat of calorimeter (CMN) with liquid He^3; 2–specific heat of one calorimeter (CMN); 3–specific heat of liquid He^3, obtained as the difference between curves 1 and 2. Dashed curve–theoretical [125] with transition temperature $T_\lambda = 0.0055$°K.

(lower curve 3). The presence of such a maximum can be attributed to the transition of He^3 into the superfluid phase. The theoretical[124] plot of the specific heat against the transition temperature $T_\lambda = 0.055$°K is shown by the dashed curve in Fig. 17. The blurring of the experimental curve indicates that there is no equilibrium distribution of the temperatures in the apparatus. In this experiment, the calorimeter was a sphere compressed of CMN crystals having an average dimension 10 μ. The liquid He^3 was introduced in the pores between the crystals. There was 1 cm³ of liquid He^3 for 14 grams of CMN. The heat was introduced into the calorimeter almost homogeneously, with the aid of gamma sources installed on both sides. The temperature T was determined from the magnetic moment of the CMN in the known measuring magnetic field

$$T = \frac{A}{M}. \qquad (30')$$

The constant A was chosen such that the maximum value M_{max} observed in the CMN at the lowest temperatures corresponded to a temperature $T_{max} = 0.0032°$, in accordance with the data of Daniels and Robinson.[125]

Similar measurements[126] were made in apparatus in which CMN crystals measuring about 150 μ filled a cylinder whose height was equal to its diameter. There was 2 cm³ of liquid He^3 for 6.5 g of CMN. The temperature in these measurements was determined also in accordance with formula (30), but in accordance with their calibration, the authors assigned a value $T_{max} = 0.0018$°K to the temperature of the maximum of M. The calorimeter was heated by a wire-wound heater. It is clear that at sufficiently small measured magnetic fields the maximum of M should occur at the same temperature for a sphere as for a cylinder. Therefore the upper part of Fig. 17 shows the results of measurements of the specific heat of liquid He^3 in such a scale that the lower and the upper curves in a given vertical section have the same temperatures. Which of the given temperature scales is closer to the thermodynamic scale can be determined only by further experiments.

As seen from the upper curve 3 of Fig. 17, a faster decrease of the specific heat of He^3 begins also below 3×10^{-3}°K, but it is much less pronounced than on the lower curve 3. This can be attributed to the fact that in the second experiment the conditions were even farther from equilibrium than in the first experiment, owing to the larger dimensions of the CMN crystals and owing to the inhomogeneous heat release. In addition, according to the data of the authors of [126], the specific heat of the CMN increases with decreasing temperature even more slowly than $c \sim 1/T^2$, as was observed[125] for spherical samples and as was observed in the given investigation at temperatures above 0.008°K. At the same time, owing to the presence of the maximum of M at $T_{max} = 0.0018°$, the values of the specific heat, in this temperature scale, should increase more rapidly on approaching T_M, becoming infinite at the point $T - T_M$. All this confirms that the conditions in the second experiment were far from equilibrium.

In a detailed article,[127] the authors of the second paper[126] ignore the smeared-out maximum of the specific heat in their own experiments, and attempt to attribute the maximum in the first investigation to the presence of a maximum in the time of establishment of thermal equilibrium between the liquid He^3 and the CMN crystals. The specific heat of the He^3 being $c_1 \sim T$ and that of the CMN $c_2 \sim T^{-2}$, the time of establishment of equilibrium is equal to $\tau = Rc_1c_2/(c_1 + c_2)$ and can have a maximum only when the resistance on the boundary varies not like $R \sim T^{-3}$, but more weakly: $R \sim T^{-1}$. In addition, in the second investigation, owing to the larger dimensions of the CMN crystals, the time of establishment of equilibrium should be 30–40 times larger than in the first investigation, whereas the authors regard their experiments as being performed under conditions close to equilibrium. It must therefore be recognized that the explanations of the authors of [127] are contradictory. In any case, their conclusion that a deviation from the linear temperature dependence of the specific heat of liquid He^3 begins below 0.01°K must be recognized as being not verified experimentally. For a more reliable establishment of the temperature dependence of the specific heat of liquid He^3 at temperatures below 0.01°K, and also for a more reliable observation of the transitions of He^3 into the superfluid phase, it is necessary to perform experiments that ensure conditions closer to equilibrium, and to use a thermometer having a lower Curie temperature and a smaller relaxation time, for example, a nuclear thermometer. Unfortunately, such experiments are very complicated.

When the He^3 goes over into the superfluid phase, ordering of the magnetic moments begins, i.e., a change in its magnetic susceptibility.[124] Experiments aimed at observing the dependence of the magnetic susceptibility of liquid He^3 on the temperature were performed by the same authors[127] as the experiments with the specific heat.[126] According to these data, from 10 to 3.5 mdeg the susceptibility is practically independent of the temperature. It is clear from Fig. 17 that, in the temperature scale employed by the authors, a decrease of susceptibility connected with the transition of the liquid He^3 into the superfluid phase should be expected at temperatures below 3 mdeg. The magnetic susceptibility of He^3 has not yet been measured at these temperatures.

Osgood and Goodkind[128] report in a recent paper that they cooled liquid He^3 to approximately 0.004°K by nuclear adiabatic demagnetization of copper. However, owing to the low accuracy of the results and the lack of reliability of the temperature, these experiments likewise do not give a definite answer. The value of the specific heat, when the temperature is reduced from 0.05°K, has a tendency to decrease rapidly, but the magnetic susceptibility remains practically unchanged.

It is therefore very desirable to experiment further at the lowest temperatures; this would make it possible to establish more accurately the temperature of the transition of He^3 into the superfluid phase, all the more since theoretical calculations show that He^3 should go over into the superfluid phase at sufficiently low temperatures.[129, 130]

19. THEORETICAL ESTIMATES

Helium has the simplest atom, and from this point of view helium is the most convenient object for the construction of a condensed-state theory capable of generalizing and explaining the available experimental data. At the present time, we are still far from the construction of general theory of the condensed state, but under certain conditions several properties of helium can already be explained theoretically qualitatively and quantitatively. The properties that can be calculated most accurately are those of weak solutions of He^3 in He^4, where the He^3 atoms move in the superfluid He^4 as in an ideal liquid, without experiencing any friction, but having a large effective mass m, equal to 2.4 the mass of the He^3 atom. The He^3 atoms interact with each other weakly and constitute, as it were, an ideal Fermi gas.

As is well known,[131] for a Fermi gas with spin 1/2 the distribution of the particles with respect to the momenta p is given by the formula

$$dN = \frac{vp^2\,dp}{\pi^2\hbar^3\left(e^{\frac{\varepsilon-\mu}{kT}}+1\right)}, \tag{31'}$$

where v is the volume, $\hbar$ is Planck's constant, k is Boltzmann's constant, μ is the chemical potential, $\varepsilon = p^2/2m_{eff}$ is the energy of the He^3 atom, and $m_{eff} = 2.4\, m_{He^3} = 1.2 \times 10^{-23}$ g.

The degeneracy temperature of the s

$$T_d = \frac{(3\pi^2 n\nu)^{2/3}\hbar^2}{2m_{eff}\,k}, \tag{32}$$

where n is the number of helium atoms per cm^3, and ν is the molar concentration of the He^3 in the solution. At temperatures much higher than T_d, formula (31) differs little from a Boltzmann distribution. In this case the specific heat per cm^3 of solution will be practically constant, just as the specific heat of an ideal gas, and will equal

$$c = \frac{3}{2} knv. \tag{33}$$

At $\nu = 0.05$ we have $T_d = 0.34$°K and, as seen from Fig. 10, when $0.6 > T > 0.2$°K the specific heat of a 5% solution is actually almost constant and agrees with formula (33). At higher temperatures, the specific heat of He^4, which is negligibly small below 0.6°K, begins to

make an appreciable contribution. There is no talk of the thermoconductivity and the viscosity of the "gas" under these conditions, since at temperatures 0.3–0.7°K they are much smaller than the thermal conductivity and viscosity of the normal part of liquid He^4. At temperatures much lower than T_d for the solution of He^3 in He^4, which exists, as seen in Fig. 3, up to concentrations $\nu \sim 0.06$ and at 0°K, the laws governing the degenerate Fermi gas should be valid. In this case the specific heat is

$$c_d = \frac{\pi^2 n \nu k T}{2 T_d}. \quad (34)$$

At $\nu = 0.05$ we have $c_d = 120$ T J/mole-deg (per mole of He^3 atoms). Using Stoner's tables,[132] we can determine the specific heat in the entire temperature region from 0°K to $T = 2T_d$.

It is seen from Fig. 10 that when T is lower than 0.05°K the specific heat of 5% solution of He^3 is actually proportional to T and agrees with formula (34).

In the degenerate state, the velocity of the particles depends very little on the temperature and is equal to

$$v_F = \sqrt{\frac{2kT_d}{m_{eff}}} = 7.6 \cdot 10^3 \nu^{1/3} \text{ cm/sec} \quad (35)$$

The order of magnitude of the mean free path can be defined as[133]

$$l_d = \frac{1}{n\nu\sigma}\left(\frac{T_d}{T}\right)^2, \quad (36)$$

where $\sigma = 5 \times 10^{-15}$ cm^2 is the gas-kinetic cross section for the scattering of the He^3 atoms. The viscosity is in this case

$$\eta_d = \frac{m_{eff} v_F n \nu}{3} = \frac{m_{eff} v_F T_d^2}{3\sigma T^2}, \quad (37)$$

and the thermal conductivity

$$\varkappa_d = \frac{C_d v_F l_d}{3} = \frac{\pi^2 v_F k T_d}{6\sigma T} \quad (38)$$

and the self diffusion is

$$D = \frac{v_F l_d}{3} = \frac{v_F T_d^2}{n\sigma\nu T^2}. \quad (39)$$

At $\nu = 0.05$, for He^3 in liquid helium, η_d (poise) $= 2.6 \times 10^{-7}/T^2$, $\varkappa_d$ (W/cm-deg) $= 4.4 \times 10^{-6}/T$, and D (cm^2/sec) $= 5.9 \times 10^{-5}/T^2$.

The results of more accurate theoretical calculations by Bardeen et al.[134] and by Emery,[135] based on experimental data[62] on the diffusion of nuclear spins in solutions of He^3 in He^4, are given in Table IV. Table IV lists also the values of the specific heat of solutions of He^3 in He^4, obtained by Abel et al.[136] For $\nu = 0.05$, the relation $\varkappa \sim T^{-1}$ begins to hold starting with 0.009°K, and for $\nu = 0.013$ starting with 0.007°K. It is possible that the values obtained by the authors for the specific heat are too low, since the average concentration in the measured interval, owing to thermoosmosis, can be much lower. In addition, the measurement of the temperature by determining the magnetic susceptibility of a cylindrical CMN sample with height equal to its diameter, as was done in this investigation at temperatures close to the Curie temperature, raises some doubts. It is seen from Table IV, however, that the theoretical estimates based on formulas (37)–(39) and the experimental values are of the same order of magnitude. The relatively larger value of D compared with $\varkappa$ can be connected with the fact that an interaction, analogous to that which leads to spin waves, exists between the magnetic moments of the He^3 nuclei.

Table IV

	$\nu = 0.013$, exp.	$\nu = 0.013$, theor	$\nu = 0.05$, exp.	$\nu = 0.05$, theor
DT^2, 10^{-5} cm^2/sec	1.72 [62]	1.72	9 [62]	9
$\varkappa T$, erg/cm-sec	11 [136]	19.1	24 [136]	64
ηT^2, 10^{-8} poise		66		75

On the basis of the experimental data, Bardeen et al.[134] calculated theoretically that, in a solution of He^3 in the superfluid state, superfluidity appears also in a "gas" consisting of He^3. According to their data, when $\nu = 0.05$ the transition temperature should lie near $T_c = 5 \times 10^{-9}$°K, and when $\nu = 0.013$ $T_c = 2.0 \times 10^{-6}$°K. The optimal concentration is $\nu = 0.016$, for which $T_c = 2.2 \times 10^{-6}$°K.

The theory of an ideal Fermi gas cannot be applied to liquid He^3. The strong interaction causes the degeneracy temperature to be only 0.5°K, instead of the 5°K given by calculation with the aid of formula (32).

Landau[137] developed a theory of the Fermi liquid, based on the assumption that while it is impossible to consider individual He^3 atoms at sufficiently low temperatures (T < 0.05°K), it is possible to consider weakly interacting excitations that are located in the self-consistent field of other excitations, the number of which is equal to the number of atoms. In this case, the energy of the entire system is no longer equal to the sum of the energies of the individual particles, and is a functional of the distribution function. However, for the function $n(\varepsilon)$ the Fermi distribution

$$n(\varepsilon) = [e^{(\varepsilon-\mu)/kT} + 1]^{-1} \quad (40)$$

remains valid, but in this case ε, being a functional of $n(\varepsilon)$, depends on the temperature.

The effective mass of the quasiparticles is determined by the relation

$$m_{eff} = \frac{p_0}{d\varepsilon/dp} = \frac{p_0}{v_F}, \quad (41)$$

where p_0 is the end-point momentum of the Fermi distribution of the quasiparticles at absolute zero, and v_F is the Fermi velocity of the quasiparticles.

The specific heat of the Fermi liquid is

$$C = \left(\frac{\pi}{3n}\right)^{2/3} \frac{m_{eff} n k^2 T}{\hbar^2}, \quad (42)$$

where n is the number of particles per unit volume.

Abrikosov and Khalatnikov,[2] and also Hone,[138] calculated the specific heat, viscosity, magnetic-moment diffusion, magnetic susceptibility, and speed of sound on the basis of the Landau theory of the Fermi liquid. Hone[138] presents a table of the parameters of liquid He^3, calculated on the basis of the experimental data on the density, magnetic susceptibility, and speed of sound. Table V gives a number of the parameters calculated by Hone, and also the Fermi velocity of the quasiparticles.

Table V

Pressure, atm	0	2.75	7.75	16,5
ρ, g/cm^3	0.082	0.089	0.097	0.106
$p_0/\hbar$, 10^{-8} cm^{-1}	0.785	0.808	0.831	0.856
m_{eff}/m	2.82	3.06	3.40	4.04
$v_F = p_0/m_{eff}$, m/sec	58.6	55.5	51.4	44.6
c, m/sec	182	223	276	335
ηT^2, poise-deg^2 theor.	$1.5\cdot10^{-6}$	$1.2\cdot10^{-6}$	$0.87\cdot10^{-6}$	$0.73\cdot10^{-6}$
ηT^2, poise-deg^2 exp. [119]	$3.2\cdot10^{-6}$			
$\varkappa T$, erg/cm-sec theor.	57	45	30	24
$\varkappa T$, erg/cm-sec exp.	48			
DT^2, cm^{2}deg^{2}sec theor.	$4.2\cdot10^{-6}$	$2.9\cdot10^{-6}$	$1.5\cdot10^{-6}$	$0.85\cdot10^{-6}$
DT^2, cm^{2}deg^{2}sec exp. [95]	$1.5\cdot10^{-6}$	$1.0\cdot10^{-6}$	$0.62\cdot10^{-6}$	$0.35\cdot10^{-6}$

As seen from Table V, there is agreement with the small amount of available experimental data. However, owing to the presence of magnetic impurities, the experimentally-obtained spin diffusion is as a rule overestimated, and therefore the discrepancy is appreciable.

One of the greatest successes of the Fermi-liquid theory is the predicted existence of zero sound.[53] At low temperatures, the relaxation time is $\tau \sim 10^{-12} T^{-2}$ sec, and therefore very large attenuation should be observed at higher temperatures for ordinary sound ($\omega\tau \gg 1$) at $\omega\tau \sim 1$ and, as seen from Fig. 7, weakly damped acoustic oscillations, called by Landau zero sound, should be observed again at $T < 0.01°K$ and $\omega\tau \ll 1$ in liquid He^3. A feature of zero sound is that whereas ordinary sound corresponds to oscillations of the radius and of the center of the Fermi sphere, zero sound is connected principally with periodic deformations of the Fermi sphere along the sound-propagation direction. This phenomenon was already described in greater detail by Pitaevskiĭ.[139]

Thus, it can be concluded that the Fermi-liquid theory explains quite satisfactorily the properties of liquid He^3 at temperatures lower than 0.05°K and down to the transition into the superfluid phase.

The main properties of liquid He^3 have been investigated experimentally above 0.05°K, and there is a wide scope here for the activity of the theoreticians.

20. USE OF He^3 TO OBTAIN VERY LOW TEMPERATURES

Inasmuch as He^3 has the lowest boiling temperature it is possible, by simple pumping of its vapor in cryostats described in the literature,[140-142] to obtain and maintain temperatures from 3° to 0.3–0.2°K. However, the singularities of the diagram of state of He^3 and of its solutions in He^4 make it possible to obtain temperatures that are much lower.

One of the methods, proposed by London et al.[143] and realized most successfully by Neganov et al.,[144] consists of using the heat of the transition of He^3 from a phase rich in He^3 into a phase rich in He^4. As seen from Fig. 3, at temperatures below 0.88°K the solutions of He^3 in He^4 become laminated into two phases—a light one, containing essentially He^3, and a heavy one, in which the main part is He^4. There are still no exact data on the heat of transition of He^3 for one phase to the other, but if we use the thermodynamic relation

$$q = T(S_1 - S_2) \tag{43}$$

and recognize that at very low temperatures the entropy of He^3 in solution, in accordance with formula (34), is numerically equal to the specific heat, i.e., $S_1 = 103\ T$ J/mole-deg when $\nu = 0.64$, and that the entropy of the second phase is practically equal to the entropy of pure He^3, i.e., $S_1 = 17\ T$ J/mole-deg, then at $T < 0.05°K$ the heat of transition is

$$q = 86T^2 \text{ J/mole} \tag{44}$$

Using (43) and Stoner's tables,[132] we can calculate the entropies and the heats of the transition with an accuracy that is determined by the data on the lamination curve of the solutions of He^3 in He^4. These quantities are listed in Table VI.

The experimental setup for obtaining very low temperatures is shown in Fig. 18. A diffusion pump 1 and a rotary pump 2 are used to pump out and compress He^3 of concentration close to 100%. The He^3 is cooled then in bath with liquid nitrogen and condensed in a capillary by heat exchange with a bath of liquid He^4 (4). It then flows through a thin capillary (5), acquires a pressure close to zero, is cooled in an evaporation bath (6) and

Table VI. Entropy of He^3 in laminated solutions and heat

T, °K	ν_1	ν_2	S_{He^3}, J/mole-deg	S_{sol}, J/mole-deg	q, J/mole	T, °K	ν_1	ν_2	S_{He^3}, J/mole-deg	S_{sol}, J/mole-deg	q, J/mole
0	5.00	7.00	0	0	0	0.25	2.48	4.55	4.0	14.8	2.70
0.025	4.93	6.96	0.4	2.6	0.055	0.30	2.13	4.07	4,6	15.8	3.36
0.050	4.73	6.83	0.8	5.0	0.21	0.35	1.85	3.67			
0.075	4.48	6.63	1.3	7.0	0.43	0.40	1.62	3.30			
0.100	4.13	6.40	1.7	9.0	0.73	0.45	1.44	2.99			
0.125	3.80	6.14	2.0	10.6	1.07	0.50	1.30	2.72			
0.150	3.47	5.79	2.4	11.9	0.42	0.55	1.19	2.48			
0.175	3.18	5.47	2.9	12.9	1.75	0.60	1.08	2.26			
0.2	2.92	5.10	3.3	13.6	2.06						

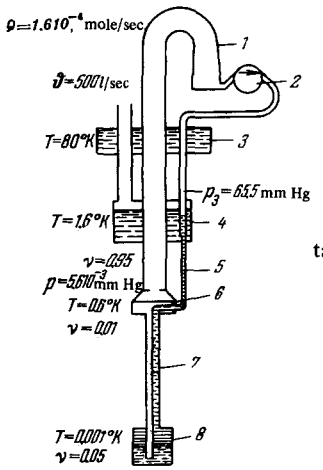

FIG. 18. Diagram of device for obtaining very low temperatures.

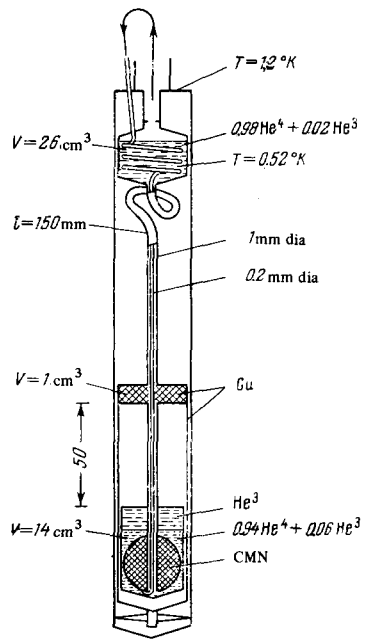

FIG. 19. Cryostat for one-time operation, based on the heat of transition of He^3 in solution.

in a heat exchanger (7), and proceeds to the upper part of the dissolution bath (8). In the dissolution bath the He^3 evaporates, as it were, into the lower phase, from which the "gaseous" He^3 proceeds by viscous flow under the influence of the concentration difference to the evaporation bath (6), where it is evaporated and pumped out with the pumps, thus closing the cycle. In order to cause the He^3 to move from the region of low temperatures into the region of higher temperatures, it is necessary to overcome the thermoosmosis forces. Table VI and the lower left part of Fig. 3 show the dependence of ν on T, corresponding to dynamic equilibrium of the thermoosmosis forces. Therefore at $\nu = 0.05$ and at low temperatures, in order to extract He^3 at $T = 0.6°K$ it is necessary to have a concentration lower than $\nu = 0.01$. The calculations for the operation of such a cryostat have been published[145] and shows that its cooling capacity W at a temperature T is

$$W(\mathbf{W}) = 43T^2 Q \text{ mole/sec} \qquad (45)$$

where Q is the rate of circulation of the He^3 in moles per second. The working temperature is determined in this case by the relation

$$T°\text{K} = 18\left(\frac{Q}{P}\right)^{0.5}, \qquad (46)$$

where P is the area of heat exchanger (7) in cm^2 and Q is in moles per second. The numerical data on Fig. 18 describe one of the calculated modes with a heat-exchanger (7) having an area $P = 5 \times 10^4$ cm^2. The cooling capacity of such a regime is only 5 erg/min. It is clear that it is impossible to ensure such a small influx of heat, taking into account the appreciable thermal conductivity of the He^3 itself and its solutions, and the presented figures should be regarded more readily as the temperature limit below which the cryostat will not operate in practice.

When the He^3 goes over from the evaporation bath (8), at a concentration 0.05, into the evaporation bath (4), with concentration 0.01, approximately 13 J/mole is absorbed, and the He^3, which flows downward in the heat exchanger, carries only 1.7 J/mole. Therefore the He^3 rising in the heat exchanger (7) has a temperature close to the temperature of the dissolution bath practically all the way to the evaporation bath. To compensate for the cold flowing downward, and also for the heat of evaporation of He^3 at a circulation 1.6×10^{-4} mole/sec, it is necessary to release approximately 6 mW in the evaporation bath.

A cryostat for one-time operation, without a complicated heat exchanger, is shown in Fig. 19. A solution of He^3 in He^4 with approximately 30% concentration is first condensed in it, after which circulation begins and lowers the temperature. After a temperature 0.6–0.7°K is reached in the evaporation bath, the heater of the evaporation bath is turned on, and the temperature of the latter is maintained constant. The almost pure He^3 becomes recondensed in the dissolution bath, and after the entire phase that is rich in He^3 is pumped over from the evaporation bath, rapid cooling of the dissolution bath begins. At the same time an amount of He^3 is added through the internal capillary, sufficient to fill the entire dissolution bath, after which, continuing the circulation, the temperature of the dissolution bath is lowered to 0.06°K, after which the circulation stops and pumping of the vapor begins from both the inlet and the outlet. As the He^3 is pumped off, the dissolution-bath temperature drops to a value established by the heat influx. Temperatures lower than 0.006°K were obtained and maintained for 30 minutes in the device shown in Fig. 19.

Vilches and Wheatley[146] produced a setup with a preliminary cooling cycle effected by dissolution and circulation of He^3. With the aid of the first stage, using superconducting switches, the second stage, designed for one-time operation, was cooled to T = 0.03°K, after which the switches were disconnected, the gas was pumped out from the evaporation bath of the second stage. They succeeded in obtaining a temperature of approximately 0.0045°K and in maintaining it for about 30 minutes. It should be noted that according to the temperature scale employed by the American authors, the temperature is assumed to be lower by a factor of 1.8.

One more method of obtaining low temperatures with the aid of He^3, a crystallization method, was proposed

by Pomeranchuk[133] and realized by Anufriev.[82] As seen from Fig. 12, the maximum cooling capacity of such a process is 0.3 J/mole at T = 0.25°K. At lower temperatures, the crystallization heat is

$$q = RT\left(1-\frac{T}{0.25}\right)\ln 2. \qquad (47)$$

The process of crystallization by pressure is connected with deformation of the crystals, and may be accompanied by appreciable heat release. If this difficulty is ever circumvented, then, excluding nuclear demagnetization, characterized by very long times required to establish thermal equilibrium between the lattice and the system of nuclear spins, the process of crystallization of He^3 makes it possible in principle to obtain temperatures $\ll 0.001°K$.

For one-time processes, when the refrigerant is cooled to a definite low temperature and then draws heat from the investigated sample, it is advantageous to compare the cooling capacity contained in one cm^3 of the refrigerant.

Let us consider processes that take place in the optimal regime, in which, following the attainment of a specified temperature, further demagnetization, crystallization, or pumping of He^3 occur at a constant temperature T. In this case the maximum cooling capacity is defined as $q = T\Delta S$, where ΔS is the difference between entropies at the beginning and at the end of the process. Table VII lists data on the maximum entropy difference between two phases and on the cooling capacity per cm^3 of different substances: ammonium ferric alum $MH_4Fe(SO_4)_4 \cdot 12H_2O$ (AFA), cerium–magnesium nitrate $Ce_2Mg_3(MO_3)_{12} \cdot 24H_2O$ (CMN), copper, liquid He^3 in crystallization (He^3_c) and the transition of He^3 from one liquid phase to the other ($He^3 \rightarrow He^4$). It is seen from the table that nuclear demagnetization ensures, at low temperatures, approximately the same cooling capacity as crystallization of He^3. It must be taken into account, however, that nuclear demagnetization cools the system of nuclear spins, and that this cold must be transmitted through the crystal lattice to other bodies, making this process quite difficult. Thus, when T = 0.001°K and the thickness of the cooled layer of liquid He^3 on copper is one micron, the time necessary to establish thermal equilibrium is on the order of 4200 sec, i.e., more than one hour, as a result of the Kapitza jump. In general, at millidegree temperatures, the question of establishment of thermoequilibrium is of decisive significance. In the absence of a magnetic field, the specific heat of metals is approximately one-thousandth the specific heat of liquid He^3, and therefore the time required to cool them with helium is shorter by a factor 1000, thus facilitating their use as thermometers.

Thus, owing to the better heat-transfer conditions, and also owing to the possibility of working in magnetic fields, the use of He^3 as a refrigerant is clearly preferable. In addition, down to temperatures on the order of several millidegrees in an He^3 dissolution cryostat it is possible to realize a continuous removal of heat at the very lowest level, regardless of the presence of the magnetic field ($H < 10^6$ G), which is also an undisputed advantage.

Therefore the statement made by Abel et al.[127] that "it is impossible to attain a larger temperature change in liquid He^3 by changing any external parameters that influence the state of the He^3" must be regarded as erroneous and, to the contrary, the use of He^3 is recommended for the production and maintenance of the very lowest temperatures, at any rate when speaking of a real temperature, i.e., when a state close to thermal equilibrium is desired.

Table VII. Cooling capacity per cm^3 of refrigerant

T, °K	AFA	CMN	Copper	Hc^3_c	$He^3 \rightarrow He^4$
			ΔS_{max}, J/cm³deg		
	0.053	0.0156	$2.2\cdot10^{-15}H^2T^{-2} - 2.8\cdot10^{-30}H^4T^{-4}$	$0.22(1-T/0.25)$	$2.4T$
			$q = T\Delta S$, erg/cm³		
	$T=0,3$ °K, $H=10$ KG		$T=0,01$° K, $H=100$ kG		
0.05	1300	7000		88 000	60 000
0.005		550	9600	11 000	600
0.0002			380	440	1

CONCLUSION

We attempted in this review to describe, on the basis of the most reliable experimental data, the main properties of He^3 and, to a certain degree, its solutions in He^4. In addition, we estimated the advantages of using He^3 to obtain the very lowest temperatures. Naturally, a review of this size cannot claim an exhaustive exposition of the known properties of He^3, but it is seen from the presented material that the experimental data with respect to the main properties of He^3 are available for temperatures higher than 0.05°K, but there is no theory capable of explaining them qualitatively or quantitatively. In the region 0.05–0.006°K, the Landau Fermi-liquid theory gives a qualitative and a quite good quantitative description of the experimental data. Many new phenomena, particularly zero sound, were predicted on its basis. The experiments in this region are not very reliable, principally owing to the lack of thermal equilibrium and the lack of good thermometers, and also to the absence of a temperature scale coinciding with the thermodynamic scale. Below 0.006°K there are only very few experiments, and all were performed under conditions not very close to thermal equilibrium. At the same time it is precisely in this region that the most interesting phenomena, connected with the transition of He^3 into the superfluid phase, are to be expected. This question is particularly interesting, since one should expect in superfluid He^3 the manifestation of the same quantum laws that appear in superconductivity of electrons in metal, but here there is no crystal lattice and the phenomena should be observed in a simpler and, if we can use the expression, purer form.

---

[1] J. G. Daunt, Adv. Phys. 1, 209 (1952).

[2] A. A. Abrikosov and I. M. Khalatnikov, Repts. Progr. Phys. 22, 329 (1959); also Usp. Fiz. Nauk 66, 177 (1958) [Sov. Phys.-Usp. 2, 68 (1959)].

[3] V. P. Peshkov and K. N. Zinov'eva, Repts. Progr. Phys. 22, 504 (1959); also Usp. Fiz. Nauk 67, 193 (1959) [Sov. Phys.-Usp. 2, 82 (1959)].

[4] J. G. Daunt, Helium Three, Ohio State Univ. Press, Columbus, 1960.
[5] E. R. Grilly and E. F. Hammel, Progr. Low Temp. Phys. 3, 113 (1960).
[6] K. W. Taconis, Progr. Low Temp. Phys. 3, 152 (1960).
[7] N. Bernadres and D. F. Brewer, Rev. Mod. Phys. 34, 190 (1962).
[8] D. F. Brewer, Progr. Cryog. (London), 27 (1964).
[9] J. G. Daunt and D. O. Edwards, Ann. Rev. Phys. Chem. 15, 83 (1964).
[10] W. E. Keller, Helium-3 and Helium-4, Plenum Press, 1966.
[11] D. Pines, The Theory of Quantum Liquids, v. 1, New York, Amsterdam, Benjamin, 1966.
[12] E. C. Kerr, Phys. Rev. 96, 551 (1954).
[13] V. P. Peshkov, Zh. Eksp. Teor. Fiz. 33, 833 (1957) [Sov. Phys.-JETP 6, 645 (1958)].
[14] R. B. Grilly and R. L. Mills, Ann. Phys. 8, 1 (1959).
[15] J. E. Rives and H. Meyer, Phys. Rev. Lett. 7, 217 (1961).
[16] E. J. Walker and H. A. Fairbank, Proc. LT-7, Toronto, 1961, p. 618.
[17] A. F. Shuch and R. L. Mills, Phys. Rev. Lett. 6, 596 (1961).
[18] T. P. Ptukha, Zh. Eksp. Teor. Fiz. 34, 33 (1958) [Sov. Phys.-JETP 7, 22 (1958)].
[19] F. G. Brickwedde, J. Res. N.B.S. A64, 1 (1960).
[20] V. P. Peshkov and A. P. Borovikov, Zh. Eksp. Teor. Fiz. 50, 844 (1966) [Sov. Phys.-JETP 23, 559 (1966)].
[21] J. H. Vignos and H. A. Fairbank, Phys. Rev. Lett. 6, 265 (1961).
[22] F. G. Brickwedde, Physica, Suppl. 24, 128 (1958).
[23] R. H. Sherman, S. G. Sydoriak, and T. R. Roberts, J. Res. N.B.S. A68, 579 (1964).
[24] R. H. Sherman and F. J. Edeskuty, Ann. Phys. 9, 522 (1960).
[25] B. N. Esel'son and N. G. Bereznyak, Zh. Eksp. Teor. Fiz. 30, 628 (1956) [Sov. Phys.-JETP 3, 568 (1956)].
[26] V. P. Peshkov and V. N. Kachinskiĭ, ibid. 31, 720 (1956) [4, 607 (1957)].
[27] H. Sommers, Phys. Rev. 88, 113 (1952).
[28] S. G. Sydoriak and T. R. Roberts, Phys. Rev. 118, 901 (1960).
[29] K. N. Zinov'eva and V. P. Peshkov, Zh. Eksp. Teor. Fiz. 37, 33 (1959) [Sov. Phys.-JETP 10, 22 (1960)].
[30] D. Edwards, D. Brewer, P. Seligman, M. Skertic, and M. Yaqub, Phys. Rev. Lett. 15, 773 (1965).
[31] A. Anderson, W. Roach, R. Sarvinski, and J. Wheatly, Phys. Rev. Lett. 16, 263 (1966).
[32] B. N. Esel'son, V. G. Ivantsov, and A. D. Shvets, Zh. Eksp. Teor. Fiz. 42, 944 (1962) [Sov. Phys.-JETP 15, 651 (1962)].
[33] D. O. Edwards, A. S. McWilliams, and J. G. Daunt, Phys. Rev. Lett. 2, 195 (1962).
[34] K. N. Zinov'eva, Zh. Eksp. Teor. Fiz. 44, 1837 (1963) [Sov. Phys.-JETP 17, 1235 (1963)].
[35] I. V. Bogoyavlenskiĭ, N. G. Bereznyak, and B. N. Esel'son, ibid. 47, 480 (1964) [20, 318 (1965)].
[36] C. Le Pair, K. W. Takonis, R. Ouboter, P. Das, and E. De Jong, Physica 31, 764 (1965).
[37] V. P. Peshkov, Zh. Eksp. Teor. Fiz. 33, 833 (1957) [Sov. Phys.-JETP 6, 645 (1958)].
[38] C. Cuthbertson and M. Cuthbertson, Proc. Roy. Soc. A135, 40 (1932).
[39] H. E. Johns and J. O. Wilhelm, Canad. J. Res. A16, 131 (1938).
[40] C. Boghosian, H. Meyer, and J. E. Rives, Phys. Rev. 146, 110 (1966).
[41] E. C. Kerr and R. D. Teyler, Ann. Phys. 20, 450 (1962).
[42] J. W. Stewart, Phys. Rev. 129, 1950 (1963).
[43] K. N. Zinov'eva, Zh. Eksp. Teor. Fiz. 29, 899 (1955) [Sov. Phys.-JETP 2, 774 (1956)].
[44] J. F. Allen and A. D. Misener, Proc. Cambr. Phil. Soc. 34, 299 (1938).
[45] C. J. Hoffman, E. J. Edeskuty, and E. F. Hammel, J. Chem. Phys. 24, 124 (1965).
[46] D. F. Brewer, A. J. Symonds, and A. L. Thomson, Phys. Lett. 13, 298 (1964).
[47] M. C. Judhram, E. Long, and L. Meyer, Phys. Rev. 97, 1453 (1955).
[48] H. L. Laquer, S. G. Sydoriak, and T. R. Roberts, Phys. Rev. 113, 417 (1959).
[49] K. R. Atkins and H. Flicker, Phys. Rev. 116, 417 (1959).
[50] J. H. Vignos and H. A. Fairbank, Phys. Rev. 147, 185 (1966).
[51] W. R. Abel, A. C. Anderson, and J. C. Wheatly, Phys. Rev. Lett. 17, 74 (1966).
[52] G. O. Harding and J. Wilks, Proc. LT-7, Toronto, 1961, p. 647.
[53] L. D. Landau, Zh. Eksp. Teor. Fiz. 32, 59 (1957) [Sov. Phys.-JETP 5, 101 (1957)].
[54] B. E. Keen, P. W. Matthews, and J. Wilks, Phys. Lett. 5, 5 (1963).
[55] K. R. Atkins and H. Flicker, Phys. Rev. 116, 1063 (1959).
[56] H. A. Fairbank, Nuovo Cimento, Suppl. 9, 325 (1958).
[57] V. P. Peshkov, Zh. Eksp. Teor. Fiz. 38, 799 (1960) [Sov. Phys.-JETP 11, 580 (1960)].
[58] T. R. Roberts and S. G. Sydoriak, Phys. Rev. 98, 1672 (1955).
[59] D. F. Brewer, J. G. Daunt, and A. K. Srecdhar, Phys. Rev. 115, 836 (1959).
[60] M. Strongin, G. O. Zimmerman, and H. A. Fairbank, Phys. Rev. 128, 1983 (1962).
[61] R. B. Ouboter, K. W. Taconis, C. Le Pair, and J. J. M. Beenakker, Physica 26, 853 (1960).
[62] A. C. Anderson, D. O. Edwards, W. R. Roach, R. E. Sharwiski, and J. C. Wheatly, Phys. Rev. Lett. 17, 367 (1966).
[63] M. J. Buckingham and W. M. Fairbank, Progr. Low Temper. Phys. 3, 80 (1961).
[64] M. R. Moldover and W. A. Little, Phys. Rev. Lett. 25, 54 (1965).
[65] L. Goldstein, Phys. Rev. 112, 1465 (1958).
[66] J. G. Dash, D. L. Goodstein, W. D. McCormick, and G. A. Stewart, Proc. LT-10, Moscow, 1966, p. 496.
[67] E. C. Heltemes and C. A. Swenson, Phys. Rev. 128, 1512 (1962).
[68] J. S. Dugdale and J. P. Frank, Phil. Trans. Roy. Soc. A257 (No. 1076), 29 (1964).
[69] J. Franck, Phys. Lett. 11, 208 (1964).
[70] H. Montgomery, Cryogenics 5, 229 (1965).
[71] H. Van Dijk and M. Durieux, Progr. Low Temper. Phys. 2, 431 (1957).

[72] E. C. Kerr, Phys. Rev. **96**, 551 (1954).
[73] L. I. Dana and J. Kamerlingh Onnes, Proc. Roy. Acad. Amsterdam **29**, 1061 (1926).
[74] R. Berman and J. Poulter, Phil. Mag. **42**, 1047 (1952).
[75] B. Weinstock, B. M. Abraham, and D. W. Osborne, Nuovo Cimento, Suppl. **9**, 310 (1958).
[76] C. A. Swenson, Phys. Rev. **86**, 870 (1952).
[77] R. L. Mills and E. R. Grilly, Symposium Liq. Sol. He^3, Ohio State Univ. Press, Columbus, Ohio, 1957, p. 100.
[78] D. O. Edwards, J. L. Baum, D. F. Brewer, J. G. Daunt, and A. S. McWilliams, Proc. LT-7, Toronto, 1961, p. 610.
[79] R. L. Mills, S. G. Sydoriak, and E. R. Grilly, Proc. LT-7, Toronto, 1961, p. 613.
[80] G. C. Straty and E. D. Adams, Phys. Rev. Lett. **17**, 290 (1966).
[81] B. M. Abraham, D. W. Osborne, and B. Weinstock, Phys. Rev. **98**, 551 (1955).
[82] Yu. D. Anufriev, ZhETF Pis. Red. 1 (6), 1 (1965) [JETP Lett. **1**, 155 (1965)].
[83] D. F. Brewer and J. G. Daunt, Phys. Rev. **115**, 843 (1959).
[84] B. T. Beal and J. Hatton, Phys. Rev. **A139**, 1751 (1965).
[85] H. A. Schwettman and H. E. Rorshach, Jr., Phys. Rev. **144**, 133 (1966).
[86] D. L. Husa, D. O. Edwards, and J. R. Gaines, Phys. Lett. **21**, 28 (1966).
[87] J. McDougall and E. C. Stoner, Phil. Trans. Roy. Soc. **A237**, 67 (1938).
[88] A. L. Thomson, H. Meyer, and P. N. Dheer, Phys. Rev. **132**, 1455 (1963).
[89] M. G. Richards and J. Hatton Giffard, Phys. Rev. **A139**, 91 (1965).
[90] A. L. Thomson, D. F. Brewer, and P. J. Reed, Proc. LT-10, Moscow, 1967, p. 338.
[91] R. H. Romer, Phys. Rev. **117**, 1183 (1960).
[92] H. C. Torrey, Nuovo Cimento, Suppl. **9**, 95 (1958).
[93] R. L. Garwin and H. A. Reich, Phys. Rev. **115**, 1473 (1959).
[94] R. L. Garwin and A. Landesman, Phys. Rev. **133**, A1503 (1964).
[95] J. C. Wheatly, Quantum Fluids, Ed. D. F. Brewer, North Holland, Publ. 1966, p. 198.
[96] J. R. Gaines, K. Lusczynski, and R. E. Norberg, Phys. Rev. **131**, 901 (1963).
[97] H. A. Reich, Proc. LT-7, Toronto, 1961, p. 633.
[98] G. Careri, G. Reuss, and J. M. Beenakker, Nuovo Cimento **13**, 148 (1949).
[99] I. Pomeranchuk, Zh. Eksp. Teor. Fiz. **19**, 42 (1949).
[100] I. M. Khalatnikov and V. N. Zharkov, ibid. **32**, 1108 (1957) [Sov. Phys.-JETP **5**, 905 (1957)].
[101] G. P. Ptukha, ibid. **40**, 1583 (1961) [**13**, 1112 (1961)].
[102] P. J. Bendt, Phys. Rev. **110**, 85 (1958).
[103] K. Fokkensk, W. Vermeer, K. W. Taconis, and R. B. Ouboter, Physica **30**, 2153 (1964).
[104] D. M. Lee and H. A. Fairbank, Phys. Rev. **116**, 1359 (1959).
[105] A. C. Anderson, J. I. Connolly, O. E. Vilches, and J. C. Wheatley, Phys. Rev. **147**, 86 (1966).
[106] B. Bertman, H. A. Fairbank, and C. W. White, Phys. Rev. **142**, 74 (1966).
[107] B. Bertman, H. A. Fairbank, R. A. Gueyr, and C.W. White, Phys. Rev. **142**, 79 (1966).
[108] L. P. Mezhov-Deglin, Zh. Eksp. Teor. Fiz. **49**, 66 (1965) [Sov. Phys.-JETP **22**, 47 (1966)].
[109] R. Bertman, C. L. Bounds, and S. J. Rogers, Proc. Roy. Soc. **289**, (No. 1416), 66 (1965).
[110] P. L. Kapitza, Zh. Eksp. Teor. Fiz. **11**, 1 (1941).
[111] I. L. Bekarovich and I. M. Khalatnikov, ibid. **39**, 1699 (1960) [**12**, 1187 (1961)].
[112] I. M. Khalatnikov, ibid. **22**, 687 (1952).
[113] H. A. Fairbank and J. Wilks, Proc. Roy. Soc. **231**, 545 (1955).
[114] Kuang Wei-yen, Zh. Eksp. Teor. Fiz. **42**, 921 (1962) [Sov. Phys.-JETP **15**, 635 (1962)].
[115] A. C. Anderson, J. I. Cannolly, and J. C. Wheatley, Phys. Rev. **135**, A910 (1964).
[116] W. Kranest and H. Raetteer, Ann. Phys. **43**, 520 (1943).
[117] K. Z. Zinov'eva, Zh. Eksp. Teor. Fiz. **34**, 609 (1958) [Sov. Phys.-JETP **7**, 421 (1958)].
[118] D. S. Betts, B. E. Keen, and J. Wilks, Proc. Roy. Soc. **A289**, 35 (1965).
[119] M. A. Black, H. E. Hall, and K. Thompson, Proc. LT-10, Moscow, 1967, p. 174.
[120] K. N. Zinov'eva, Zh. Eksp. Teor. Fiz. **31**, 31 (1956) [Sov. Phys.-JETP **4**, 36 (1957)].
[121] E. W. Becker, R. Musenta, and F. Z. Schmeissner, Physik **137**, 126 (1954).
[122] E. W. Becker and R. Muzenta, Z. Physik **140**, 535 (1955).
[123] V. P. Peshkov, Zh. Eksp. Teor. Fiz. **48**, 997 (1965) [Sov. Phys.-JETP **21**, 663 (1965)].
[124] T. Soda and R. Vasudevan, Phys. Rev. **125**, 1484 (1962).
[125] J. M. Daniels and F. M. Robinson, Phil. Mag. **44**, 630 (1953).
[126] W. R. Abel, A. C. Anderson, W. C. Black, and J. C. Wheatly, Phys. Rev. **147**, 111 (1966).
[127] W. R. Abel, A. C. Anderson, W. C. Black, and J. C. Wheatley, Physics 1, 337 (1965)
[128] E. B. Osgood and J. M. Goodkind, Phys. Rev. Lett. **18**, 894 (1967).
[129] L. P. Pitaevskiĭ, Zh. Eksp. Teor. Fiz. **37**, 1794 (1959) [Sov. Phys.-JETP **10**, 1267 (1960)].
[130] L. N. Cooper, R. L. Mills, and A. M. Sessler, Phys. Rev. **114**, 1377 (1959).
[131] L. D. Landau and E. M. Lifshitz, Statisticheskaya fizika, Nauka, 1964 [Statistical Physics, Addison-Wesley, 1958].
[132] E. Stoner, Phil. Mag. **25**, 899 (1938).
[133] I. Pomeranchuk, Zh. Eksp. Teor. Fiz. **20**, 919 (1950).
[134] J. Bardeen, G. Baum, and D. Pines, Phys. Rev. Lett. **17**, 372 (1966).
[135] V. J. Emery, Preprint.
[136] W. R. Abel, R. T. Johnson, and J. C. Wheatley, Phys. Rev. Lett. **18**, 737 (1967).
[137] L. D. Landau, Zh. Eksp. Teor. Fiz. **30**, 1058 (1956) [Sov. Phys.-JETP **3**, 920 (1956)].
[138] D. Hone, Phys. Rev. **125**, 1494 (1962).
[139] L. P. Pitaevskiĭ, Usp. Fiz. Nauk **91**, 309 (1967) [Sov. Phys.-Usp. **10**, 100 (1967)].
[140] V. P. Peshkov, K. N. Zinov'eva, and A. I. Filimonov, Zh. Eksp. Teor. Fiz. **36**, 1034 (1959) [Sov. Phys.-JETP **9**, 734 (1959)].

[141] A. D. Shvets, PTE No. 6, 5 (1965).
[142] D. Walton, Rev. Sci. Inst. **37**, 734 (1966).
[143] H. London, G. Clarke, and E. Mendoza, Phys. Rev. **128**, 1992 (1962).
[144] B. Beganov, N. Borisov, and M. Liburg, Zh. Eksp. Teor. Fiz. **50**, 1445 (1966) [Sov. Phys.-JETP **23**, 959 (1966)].
[145] V. P. Peshkov, ibid. **51**, 1821 (1966) [24, 1227 (1967)].
[146] O. E. Vilches and J. C. Wheatley, Phys. Lett. **A24**, 440 (1967)].
[147] E. M. Ifft, O. Edwards, R. E. Sarwinski, and M. M. Skertic, Phys. Rev. Lett. **19**, 831 (1967)].

Translated by J. G. Adashko